Photometric Search for variable stars in the field of two Northern open clusters, DOLIDGE 14 and NGC 1960

Gireesh C. Joshi (gchandra.2012@rediffmail.com)

Research Article

Keywords: Astronomical reduction , NGC 1960, DOLIDZE 14, stellar Variability

DOI: https://doi.org/10.21203/rs.3.rs-1895965/v2

Additional Declarations: No competing interests reported.

Photometric Search for variable stars in the field of two Northern open clusters, DOLIDGE 14 and NGC 1960

Gireesh C. Joshi[1]

Email:- gchandra.2012@rediffmail.com

Abstract The aim of present work is extract and analyses the light curves of the stars in the fields of two clusters, NGC 1960 and DOLIDZE 14. The photometric extraction is performed by comprehensive methodology of SSM via standard transformation and differential photometry using two comparison stars per candidate variable target. The resultant light curves for each possible variable star are displayed and their period analysis are performed via two different methods. The period and classification of 18 discovered short periodic type variable stars of NGC 1960 are discussed, which consist of **four known variable stars and fourteen new variable stars**. In the case of DOLIDZE 14, four discovered variables consist of one miscellaneous, one rotational, two *binary* type variable stars. In the case of NGC 1960, the 12 selected comparison stars seems to be possible candidate for long periodic variability and 4 stars may be standard stars. The variation in brightness of other twenty comparison stars is non-pulsating with irregular pattern. Membership analysis of variable stars are performed by using their distance, kinematic probability and location in $(U-B)$ vs $(B-V)$ TCD. **C-M diagrams were constructed to confirm the evolutionary state of the new variable stars.**

Keywords Astronomical reduction – NGC 1960, DOLIDZE 14, stellar Variability

Gireesh C. Joshi

[1]Department of Physics, Government Degree College, Kanvaghati (Kotdwar), Pauri-246149

1 Introduction

An open cluster (OCL) is loosely bounded group of up to a few thousand stars caused by the mutual gravitational attraction of cluster members. OCLs are host the stars of Pop I. The brightness fluctuations are found for some stars among members of stellar population and such stars are known to be variable stars. The stellar variability may be arise either due to intrinsic properties (pulsations, eruptions, stellar swelling and shrinking) or extrinsic reasons (eclipsed by stellar rotation by another star or planet etc.).

The variable stars are natural targets of study for any civilization due to their correlation between period and total light output, which allowed them to become the first rung in the astronomical distance ladder (Hippke et al. 2015). Pulsating variables are most important objects due to the periodic expansion and contraction of the surface layers of the stars to maintain its equilibrium. Their census including pulsators and binaries, can provide important clues to stellar evolution and the host star clusters (Luo et al. 2012). The several classes of pulsating variables are largely found at instability strip region of the Hertzsprung-Russell (HR) diagram. Since, pulsating variables has an associated instability strip (Dupret et al. 2004) above the MS, therefore, an OCL provides an opportunity to estimate the properties of its stellar variables through its own characteristic parameters.

Since the detection and magnitude estimation of the most fainter stars are primary affected by their nearby brighter stars, the knowledge of flux contamination of the stars in the science frame of any cluster is absolutely necessary to investigate the nature of instrumental pseudo-variability. In this connection, we need a cluster region fulfilled by brighter stars and NGC 1960 is found a potential candidate for such study. Other hand, deep time-series phtometry is further bound by

exposure time to investigate the variable stars within enhanced fainter stars filed of any cluster. For this purpose, DOLIDZE 14 is found a potential candidate.

In this background, we are carried out analysis of the time series observations of NGC 1960 and DOLIDZE 14 to search the variable stars within them. The previous parametric studies of both clusters are given in the Section 2. The observational details of these clusters are given in the Section 3. The methodology of data reduction is discussed in the Section 4. The identification procedure of variable stars of DOLIDZE 14 and NGC 1960 is given in the Section 5. The Fast-Fourier analysis of variables discuss in Section 6. The mean-proper motions and kinematic membership probabilities for both clusters are described in Section 7. A comparative study of variable stars with parameters of both clusters is discussed in Section 8. A detail description of identified stars of cluster DOLIDZE 14 and NGC 1960 is given in Sections 9 and 10. Results, discussion and Conclusion are described in Sections 11 & 12.

2 Previous studies and antecedents of stellar variability

2.1 NGC 1960

This cluster is situated in the Constellation Auriga and has been studied in the past by many authors. The Center coordinates ($\alpha,\ \delta$) for this cluster is estimated to be ($05^h : 36^m : 20.8^s,\ +34^o : 08^{'} : 31^{"}$) and ($05^h : 36^m : 20.2^s,\ +34^o : 08^{'} : 06^{"}$) by Sharma et al. (2006) and Cantat & Anders (2020), respectively. Its angular size is computed to be 16 arcmin and 10.3 arcmin by Joshi & Tyagi (2015a) and Cantat & Anders (2020), respectively. **Previously, the study of this cluster is done by various research groups [Barkhatatova et al. (1985), Conrad et al. (2017), Hasan et al. (2005), Jeffries et al. (2013), Johnson & Morgan (1953), Kharchenko et al. (2004) Nilakshi et al. (2002), Sanner et al. (2000), Sharma et al. (2006, 2008)]**.

A complete $UBVRIJHKW_1W_2$ photometric catalogue has been represented by Joshi & Tyagi (2015a) by complying the PPMXL catalogue with the obtained $UBVRI$ standard photometric magnitude of gathered data on date of 30 Nov, 2010 and same data set was further analyzed by JO20 for their absolute/standard photometric analysis. By utilizing catalogues of various data-sets, a comprehensive photometric analysis of this cluster along with the long-term variability is represented by them. A total of 76 variable stars of NGC 1960 has been identified by JO20, and their analysis confirmed 72 periodic variables among them, 59 are short period ($P < 1\ d$). They used absolute photometry for detection of variable stars, in which instrumental errors are surely added due to magnitude transformation. **In the case of dataset of J20, only three data strings have continuous time series observation with a gape of more than 1 yr and length of data string is less than 3.5 hours (i.e. $\simeq$ 0.146 d). time gape more than 1 yr leads additional aliases. Mostly, other observational nights contain 1-3 frames only with irregular exposure time as well as time interval, which are not seems to be suitable find out short periodic variable stars. Thus, it is impossible to determine the short periodic variable stars.**

In the case of this cluster, flux of detected nearby fainter stars of brighter stars will be contaminated during its deep CCD photometric observations. Such circumstances surely lead an over-estimation in the detection of short periodic variable stars. In the view of above antecedent, author is also motivated to perform time series observations of this cluster with low exposure times of 05, 06 and 10 seconds .

2.2 DOLIDZE 14

In the database of WEBDA, the center coordinates, $(\alpha,\ \delta)_{J2000}$, of DOLIDZE 14 is ($04^h : 06^m : 36.0^s,\ +27^o : 26^{'} : 00.0^{"}$) as per work of Alter et al. (1970). Joshi et al. (2015) has been studied nature of stellar enhancement around the celestial coordinates, ($04^h : 06^m : 36.0^s,\ +27^o : 26^{'} : 00.0^{"}$)$_{J2000}$ and they depicted results as per infrared photometric analysis of stars within DOLIDZE 14. This cluster have stellar enhancement in the B-band of USNB1.0, whereas it does not show any stellar enhancement in the infra-red bands (Joshi & Tyagi 2015b). In this connection, they have been estimated the values of ($\alpha,\ \delta$))$J2000$ and ($\mu_x,\ \mu_y$) as ($04^h : 06^m : 26.7^s,\ +27^o : 22^{'} : 26.7^{"}$) and ($-0.15\pm0.34\ mas/yr,\ -7.79\pm0.41\ mas/yr$), respectively. Joshi et al. (2015) are estimated the values of radius, reddening and distance as $9.6\pm0.2\ arcmin$, $0.32\pm0.02\ mag$ and $1.67\pm0.14\ kpc$ respectively. It is a suitable field for analysis of deep CCD-photometic observations due to have a system of fainter stars and it is also non-standardized in optical photometry.

For the name of cluster DOLIDZE 14, Dias et al. (2014) gave the values of center coordinates ($\alpha,\ \delta)_{J2000}$, and proper motions ($\mu_x,\ \mu_y$) as ($04^h : 06^m : 43.0^s,\ +27^o : 32^{'} : 34.0^{"}$) and (1.71 mas/yr, -0.88 mas/yr) respectively. This given center of cluster is separated by 08 arcmin with respect to that of Alter et al. (1970) and

this cluster is denoted by $C\ 0403+273$ in the database of SIMBAD. As a result, author concludes that cluster DOLIDZE 14 [$(04^h : 06^m : 26.7^s,\ +27^o : 22^{'} : 26.7^{"})_{J2000}$] and cluster $C\ 0403+273$ [$(04^h : 06^m : 43.0^s,\ +27^o : 32^{'} : 34.0^{"})_{J2000}$] are historically distinct regions and may have cluster properties.

The nature of absolute photometry for time series observation for any cluster may be understood with respect to secondary standard stars within it and its comparative analysis can be represented using a non-standardized system of stars. As per above antecedents of DOLIDZE 14 [$(04^h : 06^m : 26.7^s,\ +27^o : 22^{'} : 26.7^{"})_{J2000}$], it is potential system of stars for such comparative analysis.

3 Data Collection and Extraction

To detect the short periodic pulsation of stars of target cluster, we need time series observation of the whole night as per availability of target in the telescopic field of view. The time series observations of studied clusters, DOLIDZE 14 and NGC 1960, are carried out by utilizing observational facilities of 1.04-m Sampurnand telescope of ARIES, Manora Peak, Nainital. The CCD camera of 1.04-m Sampunanad telescope of ARIES covers 15×15 $arcmin^2$ field of view of the target objects. Since, the size of both clusters is more than the telescopic field of view, therefore, we have performed an analysis of the time series observations of the core regions of both clusters. In this connection, the bias and flat frames are also observed for each observational night of studied clusters. The weather conditions (seeing, humidity, wind flow, passing clouds etc.) and declination of target object affect the receiving flux of stars. Thus, the quality of observational data is most important to perform the crucial task of identification of variables. In this connection, the selection procedure of exposure times and observational details of clusters are given as below,

3.1 Characteristics of observational data of NGC 1960

To identify short periodic pulsations of stars within core region of NGC 1960, time series observations are carried out in V-band during 5 observation nights (2012-2015). It contains ten stars of a visual magnitude brighter than 10 (Jeffries et al. 2013), one B-type Variable of 9^{th} magnitude (Delgado et al. 1984), 178 down to magnitude 14 (Sanner et al. 2000) and 38 members have infrared excess (Smith & Jeffries 2012). Thus, our telescopic field of view for NGC 1960 is fulfilled by several brighter stars. We found that these brighter stars almost saturated during an exposure time of 5 seconds. In this regard, the value of exposure time of 5 seconds in V-band becomes too high for saturation counts of the brighter stars of NGC 1960 and leads flux contamination for near by fainter stars of brighter stars in the observed science frames using the facility 1.04-m telescope at ARIES, Nainital. Similarly, an exposure time of 1 second is too low value to collection the stellar information for fainter stars of NGC 1960 below 17 mag in V-band. Environmental influences (seeing, air flow, humidity, passing clouds etc.) and high declination of the target cluster from zenith further reduce the value of stellar magnitude and alter the rate of stellar detection. As a result, different number of faint stars are detected in different science frames of NGC 1960. To overcome the detection problem of faint stars, author performed the deep CCD photometric observation of core region of NGC 1960, with exposure times of 10, 20 and 60 seconds. We need continuous observations of 4-6 hours or more, therefore, the science frames of NGC 1960 have been captured in the alternating order of low (5 or 6 seconds) and high (10 or 20 or 60 seconds) exposure times during the observation session of night. Thus, the exposure time plays a major role to collect the stellar information. The visual picture of science frames for exposure times of 10 and 60 seconds for NGC 1960 are shown in the right and left panels of Figure 1. In these figures, flux contamination of nearby stars of brighter stars are found more for science frame with exposure times of 60 seconds than that of 10 seconds. The detail of exposure times and brief description of present used data is given in Table 1. **After inspecting light curves of studied variable stars and their comparison star in Figures 4-9, the quality of these curves dated 24/01/2012 and 20/12/2013 is found too low to identify the nature of stellar variability. Observations with exposure time, 60 seconds,**

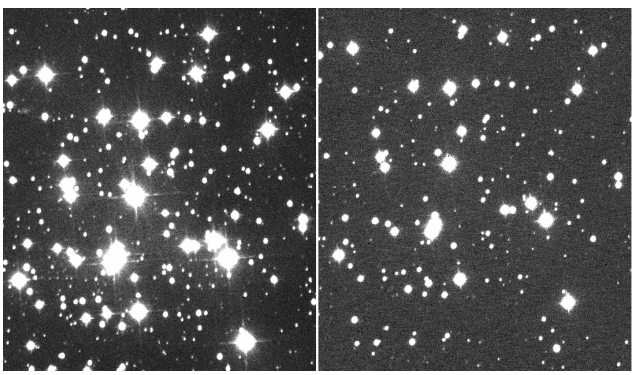

Fig. 1 In the left and right panels of this figure, the science frames of 60 seconds and 10 seconds are shown for core-region of NGC 1960, which are observed on date 24-01-2012 and 11-12-2013 respectively.

Table 1 The data dated 30/11/2012 and 24/01/2012 for NGC 1960 are common with Joshi & Tyagi (2015) and Joshi et al. (2020), respectively. In the present work, the author collected an additional data-set of 330 frames over 4 nights in the filter V with $t_{exp} = 5 - 60$ *sec* (variable). The observation details of collected data of DOLIDZE 14 and NGC 1960 for searching variable stars within them.

1. DOLIDZE 14

S.No.	Date	Observation Band (Frames)	Observation Time & Mode	No. of Frames	Exposure Time
1.	13-10-2014	I	3.25 hours, Slow	52	150 Sec.

2. NGC 1960

S.No.	Date	Observation Band (Frames)	Observation Time & Mode	No. of Frames	Exposure Time
1.	30-11-2010	U	–, Slow	002	300 Sec.
		B		002	300 Sec.
		V		002	200 Sec.
		R		002	200 Sec.
		U		002	060 Sec.
2.	24-01-2012	V	3.5 hours, Slow	070	60 Sec.
3.	11-12-2013	V (150 frames)	5.4 hours, Slow	050	05 Sec.
				050	10 Sec.
				050	20 Sec.
4.	20-12-2013	V (080 frames)	7.6 hours, Slow	040	06 Sec.
				040	60 Sec.
5.	12-01-2015	V (200 frames)	7.2 hours, Slow	100	05 Sec.
				100	20 Sec.
6.	08-02-2015	V (140 frames)	5.6 hours, Slow	140	20 Sec.

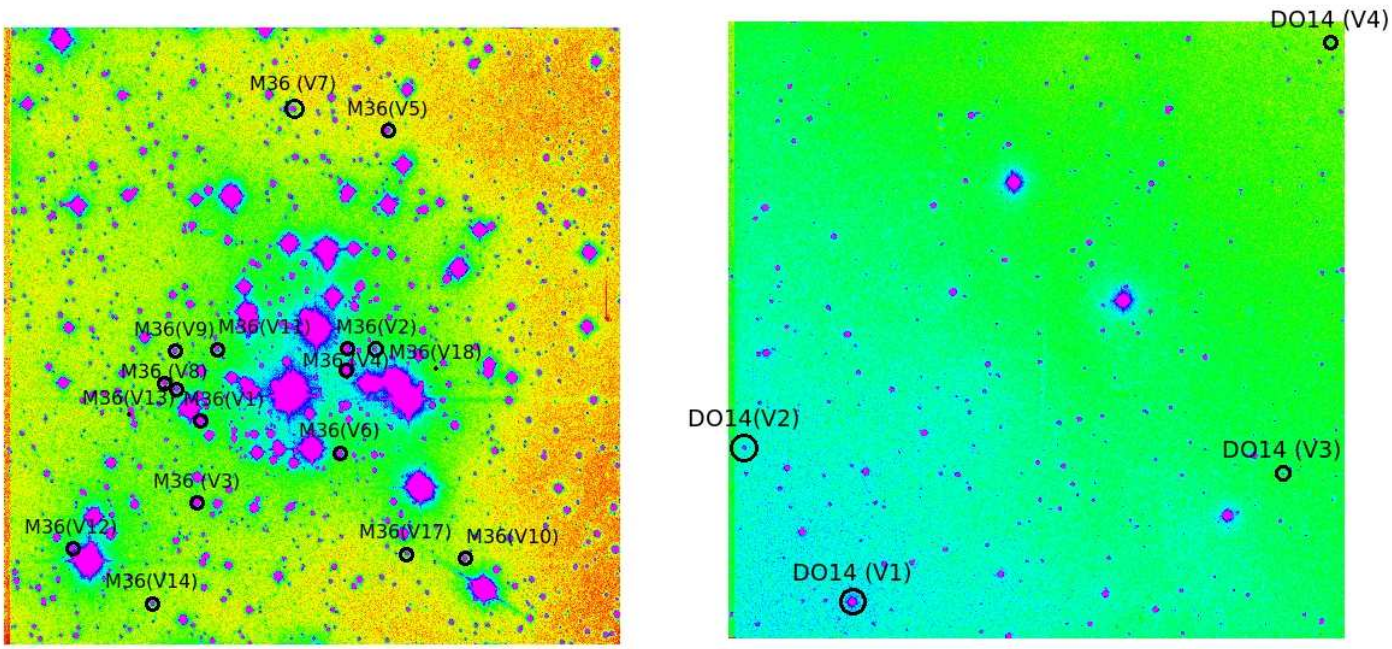

Fig. 2 In the left and right panels, the science frames are shown for core-region of NGC 1960 (M36) and DOLIDZE 14 in V-band and I-band as observed on date 30-11-2010 and 13-10-2014 respectively. The exposure times for them were taken to be 200 seconds and 150 seconds, respectively. The present detected variable stars are depicted by open circle in these Finding charts.

are performed during above dates. Thus, author concludes that observations with exposure times, 05-20 seconds, are suitable to analysis the nature of stellar variability within NGC 1960. In observational sets of 43 nights, JO20 have 1, 1 and 19 observational nights with a exposure time 40, 200 and 60 seconds, respectively. It is noted that data strings dated 02/11/2011, 03/11/2011 and 24/12/2012 include observation with exposure time 60 seconds. In this background, the classification of variable stars within NGC 1960 by JO20 is seems to be very suspicious.

3.2 Characteristics of observational data of DOLIDZE 14

The deep CCD photometric observations are needed for stellar detection in the field of view of DOLIDZE 14 due to its faintness. In this connection, this cluster is observed in I-band on the date 13 Oct, 2014 through 1.04-m Sampurnanand telescope at ARIES, Manora Peak, Nainital. A total of 52 science frames are captured over a period of 3 hours 15 min. **A high value of exposure time (200-300 seconds) is required to identify fainter stars in order to 20 mag or more.** It was noted that the positions of the stars slightly shifted during exposure time of 200-300 seconds. Consequently, the observations of longer exposure times for open cluster has been avoided. **An exposure time of 100-200 seconds is suitable to time series observation of fainter stars, with range of 14-20 mag. In this connection,** a time series observation of this cluster with an exposure time of 150 seconds is done by the author. The visual picture of science frame of DOLIDZE 14 is shown in right panel of Figure 2 and details of its observations is listed in Table 1.

4 Methodology of Data reduction

The bias correction and flat-fielding of observed science frames of NGC 1960 and DOLIDZE 14 have been carried out by using those bias and flat frames, which are observed in the same observational night of object. We are also utilized bias and flat frames of nearby night for the science frames of NGC 1960 due to the lack of these frames in observed data. For this purpose, the 'ZEROCOMBINE' and 'FLATCOMBINE' tasks of 'IRAF' package are utilized. 'COSMICRAYS' task of 'IRAF' software are used to remove cosmic rays from the science frames. 'GEOMAP' and 'GEOTRAN' tasks of IRAF software are utilized to align the all science frames for analysis. In the astrometry, pixel coordinates of detected stars have been transformed into celestial coordinates (α_{2000}, δ_{2000}) by using a linear astrometric solution as derived by matching a set of common stars between present reference catalogue and the 2MASS catalogue with the rms value of about one arcsec in RA and DEC. A total of 29 and 63 common stars are selected in the observed field of DOLIDZE 14 and NGC 1960 respectively. For this purpose, the visualization of images and access to catalogues has been done by 'SKYCAT' tool of ESO[1]. The $CCMAP$ and $CCTRAN$ tasks of $IRAF$ were used for these transformation.

4.1 standardization Details for NGC 1960

In order to perform consistent photometry from night to night on the aligned images (Joshi et al. 2012), we need a master list of stars from science frames of target cluster, which have the best seeing and coverage of the observed core region of both clusters. By using prescribed telescope in Section 3.1, the photometric observations of the open star cluster NGC 1960 were obtained on the night of 30 Nov, 2010. The bias and twilight flat frames were obtained during the observational night for the normalization of the CCD pixels. Two Landolt's standard fields $SA95$ and $PG0231+051$ (Landolt 1992) were also observed on the same observational night. A total of ten frames of the cluster with 2 frames each in U, B, V, R and I filters having exposure times of 300, 300, 200, 200 and 60-sec were obtained in respective passbands. All the observations were taken in 2 × 2 binning mode for improving the signal-to-noise ratio. The basic steps of image processing such as bias subtraction, flat fielding and cosmic-ray removal were performed through $IRAF$[2]. Photometry analysis was done using $DAOPHOT\ II$ profile fitting software (Stetson 1987). To determine the difference between aperture and profile-fitting magnitudes, the construction of an aperture growth curve was carried out by $DAOGROW$ program (Stetson 1992). The instrumental magnitude was translated into standard magnitude using the following transformation equation:

$$m_i = M_i + z_i + c_i \times color + k_i \times X \quad (1)$$

where z_i, c_i, m_i, M_i and k_i are respectively represent the zero-point, colour-coefficient, aperture instrumental

[1] www.eso.org/sci/observing

[2] Image Reduction and Analysis Facilities (IRAF) is distributed by the National Optical Astronomy Observatories, operated by the Association of Universities for Research in Astronomy Inc., under cooperative agreement with the National Science foundation.

magnitude and extinction coefficient for different pass-bands. The $(U-B)$, $(B-V)$, $(V-R)$ and $(R-I)$ colours were used to determine instrumental magnitudes in U, B, V, R and I pass-bands, while X is used for air-mass. The zero-point, colour coefficient and extinction coefficient for $UBVRI$ pass-bands are listed in Table 2.

In Fig. 3(a), author has shown the variation of standard deviations with brightness of stars in different pass-bands. It is clear from this figure that the errors are higher at the fainter end. The calibrated residuals in magnitude (difference between standard and calibrated magnitude) of standard stars in the Landolt's field are shown in Fig. 3(b). The standard deviation of the calibration are respectively estimated as 0.083, 0.071, 0.047, 0.030 and 0.049 mag in U, B, V, R and I filters. Present photometry resulted in a total of 1605 stars within $13' \times 13'$ field of the cluster NGC 1960 in which 447, 1088, 1424, 1583 and 1532 stars were found in U, B, V, R and I bands, respectively. The observed field of NGC 1960 is only central region due to the limited field of view of observation facilities. **A total of 1194 stars are found to be common between** present photometric data with the Sharma et al. (2006). **In the core region of NGC 1960, 409 additional stars are also detected in present photometry compare that Sharma et al. (2006)**

4.2 Transformation of stellar magnitude for DOLIDZE 14

It is noted that OCL, DOLDIZE 14 have not calibrated by any standardized field at yet. In this background, data set of detected stars of its first science frame of our work considered to be its reference catalogue for further analysis of stellar variability within it. Other observed science frames of DOLIDZE 14 are calibrated according to this reference catalogue by using the technique of SSM to reduce atmospheric-effect and estimation-errors of stellar magnitudes during the data collection. In this connection, we need a set of common stars, which are available in their reference frame and science frames. These common stars are used to find out a linear fit between the reference magnitudes and instrumental magnitudes of each frames, assuming that most of the stars have stable magnitude. For this purpose, we reject those stars for linear fitting, which deviate more than 3σ limit of deviations of fitting. Resultant linear solution are used to transform instrumental magnitudes of stars of studied clusters into their absolute magnitudes.

Table 2 The zeropoint, colour-coefficient and extinction-coefficient for different passbands. The colour-coefficients and extinction coefficients listed here.

Filter	zeropoint(z_i)	colour coefficient(c_i)	extinction coefficient(k_i)
U	8.16 ± 0.01	-0.05 ± 0.01	0.55 ± 0.02
B	5.81 ± 0.02	-0.01 ± 0.02	0.29 ± 0.03
V	5.43 ± 0.01	-0.08 ± 0.01	0.15 ± 0.01
R	5.23 ± 0.01	-0.09 ± 0.02	0.09 ± 0.02
I	5.63 ± 0.02	0.01 ± 0.01	0.07 ± 0.02

4.3 Secondary standardization method for NGC 1960

In the case of NGC 1960, to translate the stellar magnitudes (as extracted from data on the remaining nights) into absolute magnitudes, the differential photometry was performed using $UBVRI$ catalogue of secondary stars. For this purpose, author used a linear fit between the standard and instrumental magnitudes on each science frame, assuming that most of the stars are non-variables (these non-variable stars also called stable stars). This procedure is defined as the secondary standardization method [SSM Joshi, G.C. (2015)]. It is effective to estimate the absolute stellar magnitudes of NGC 1960 through the calibrated magnitudes of its stable stars. The magnitudes of variable stars are rapidly varying compare to other stars and identified variable stars were not utilized for such calibration. In this connection, the master list of stable stars of observed core region of NGC 1960 is prepared by using method as discussed for DOLIDZE 14.

5 Identification of variable stars

The shapes of light curves of a variable star give valuable information for examining the nature of stellar variability and underlying physical processes producing the brightness changes. As a result, the possible variable candidates identify by inspecting of their light curves (Sariya et al. 2014). If, we find the deviation of absolute magnitudes of star more than 3σ limit of mean value of its light curve, then, it will be considered a possible candidate of variable stars. The amplitude or period of the pulsations can be related to the luminosity of the pulsating stars and shape of their light curves can be an indicator of the pulsation mode (Wood & Sebo 1996). As a result, pulsating variables are distinguished by their periods of pulsation and the shapes of their light curves (Lata et al. 2014). For this purpose, the applied procedure for searching variable stars is discussed as below,

5.1 Need of Differential Photometry for searching variable stars

The collective information of variation of stellar magnitude with time is known to be light curve of target. The varying sky conditions during observations

Table 3 A complete UBVRI catalogue of the stars in the core field of the cluster NGC 1960. Columns 2 and 3 are RA and DEC of stars, respectively in epoch J(2000). From column 4 to 13, author gives photometric magnitudes and corresponding errors in $UBVRI$ passbands.

ID	RA	DEC	U	e_U	B	e_B	V	e_V	R	e_R	I	e_I
1	5:36:03.22	34:03:37.5	10.654	0.005	10.605	0.023	10.449	0.018	10.400	0.003	10.295	0.003
2	5:35:59.29	34:10:27.5	10.322	-	-	-	10.582	-	10.543	-	10.414	-
3	5:36:03.29	34:10:07.9	10.457	-	-	-	10.601	-	10.563	-	10.440	-
4	5:36:34.76	34:03:55.5	10.374	0.004	10.738	0.018	10.636	0.006	10.559	0.004	10.530	0.004
.	.	.	.	.	.	.	.	.	.	.	.	.
9	5:36:08.27	34:14:21.2	12.547	0.005	11.900	0.016	10.900	0.010	-	-	9.762	0.007
10	5:36:22.14	34:07:13.9	11.010	0.003	11.330	0.008	11.165	0.0032	11.082	0.007	11.019	0.004
11	5:36:01.97	34:09:17.7	11.148	0.004	11.382	0.016	11.212	0.007	11.117	0.003	10.999	0.003
12	5:36:15.80	34:14:18.2	11.277	0.004	11.693	0.014	11.235	0.008	10.938	0.008	10.598	0.005
13	5:36:11.54	34:07:06.5	11.145	0.003	11.496	0.009	11.340	0.003	11.274	0.007	11.210	0.005
14	5:35:51.67	34:10:32.6	11.323	0.005	11.539	0.010	11.424	0.007	11.344	0.005	11.243	0.005
15	5:36:07.75	34:09:25.2	11.642	0.003	11.751	0.016	11.524	0.006	11.387	0.004	11.218	0.004
.	.	.	.	.	.	.	.	.	.	.	.	.
.	.	.	.	.	.	.	.	.	.	.	.	.

generate noise and instrumental errors, which lead to the scattering of data points in the stellar light curves. Thus, stellar light curves carry the information of stellar variability as well as irregular variations due to instrument errors, noise and their aliases. A varied sky condition alters the equal amount of stellar fluxes for all isolated stars as detected in a science frame of target. The different orders of variation is obtained in instrumental magnitudes for stars as per their different amount of fluxes. Such variation may produce different pattern of pseudo-variability in light curves for stars, having different magnitude. Although, same pattern of pseudo-variability is found for nearby isolated stars, having approximate similar in terms of colour and magnitudes. Hence, such irregular variations have the same pattern for similar isolated stars and can be narrowed down through the differential photometry. If, the comparison stars have been chosen correctly in the case of isolated stars of field of view of any target object, then the difference between their magnitudes should be approximately constant along the night.

5.2 Limitation of Differential Photometry in present study

It is also noted that effect of contamination depends on exposure times as well as stellar distances from brighter stars. Since, the observed field of NGC 1960 is highly contaminated due to presence of brighter stars at its core region, therefore, magnitude variation for nearby stars of these bright stars is varied as per physical distance and stellar orientation. In addition, Exposure time of its science frames is not constant during observation, which further leads different amount of flux contamination for them. Eventhough, the flux contamination is also changed for same exposure time as per distance of cluster from Zenith. As a result, difference of instrumental magnitudes of nearby similar comparison stars of detected variables is not found approximately constant for NGC 1960. Since, DOLIDZE 14 is observed in I-band only, therefore, the comparison stars of its variable is searched in such a way that their I-magnitudes may closer to corresponding variables. Such detected comparison stars are found physically far away from their variable. As a result, detected comparison stars are not correctly suitable for variables of DOLIDZE 14.

5.3 Secondary standardization Methodology and transformation of stellar magnitudes

The transformation of apparent magnitude of stars into absolute magnitudes is performed through Secondary Standardization Methodology (SSM). During absolute phototmetry, there are no need of comparison stars for any variable star leads a major advantage over the differential photometry. The number of detected stars of any science frame depends on its exposure time. A total of 200±50 stars are detected in each frame for DOLIDZE 14, whereas, 1800-3000 stars are found in the science frames of NGC 1960. The absolute stellar magnitudes is computed for instrumental magnitudes of each science frame for NGC 1960 by application of SSM. Other hand, the reference frame of DOLIDZE 14 did not standardized with respect to any standard field stars. The stellar magnitudes of detected stars of each science frame of DOLIDZE 14 are translated with respect to its reference frame, therefore, SSM methodology provides the apparent stellar magnitudes for DOLIDZE 14 by considering the uniform variation in stellar magnitudes due to various sky conditions for

the entire session of observations. In these circumferences, the variables stars are detected after visual inspection of light curves as per standard magnitudes via absolute photometry. The possible candidacy of variable stars is assigned for stars, having a variation of amplitudes above the 3σ limit of its mean in light curves. After the visual inspection of light curves of detected stars of both clusters, we found a total of 4 and 18 possible variable candidates in the observed field of DOLIDZE 14 and NGC 1960, respectively.

5.4 Limitation of SSM during search of variable stars

The approximate constant environment parameter (seeing, humidity etc.) and dark night is essential conditions for standardization. The sky conditions change with unexpectedly, the transformation coefficients also vary accordingly during the process of SSM of each science frame. As a result, errors of computed stellar magnitudes in absolute photometry may be found due to aliases of different sky conditions with the estimation errors in transformation coefficients. In this connection, light curves of stars show some variation in brightness. These variations are very close to estimated stellar magnitudes with respect to standard and reference catalogue. Such variation can also produce the pseudo stellar variability.

These transformed stellar magnitudes are used to generate the light curves of stars. Only those stars has been selected as variable stars, which have magnitude variation greater than three times of estimation errors of magnitudes in their light curves as constructed after SSM approach.

5.5 Test of stellar variability via SSM and differential photometry

In the present work, we have not found ideal nearby comparison stars for detected variable stars of both clusters and we are not capable to apply only differential photometry for such case. Since, there are no available information of influence of the pseudo variability in detected variables, therefore, author also analyze light curves of stable stars, having same order of magnitudes of variables, for tracing the pattern of pseudo-variability among them.

Since, the transformation of instrumental magnitudes leads additional errors, therefore, the scattering is further increased in data points of their light curves. Such transformation makes a weak information of stellar variability. Thus, it may possible that a selected stable comparison star for any variable star have weak information of stellar variability below 3σ limit of its light curves. As a result, we have been avoided the practice of selection of a single stable star for comparing its light curve that of potential variable. For accuracy, author has selected two stable comparison stars for each potentially variable star within their science frames as observed for each cluster. It is kept in the point of view that the magnitude difference of selected comparison stars (possibly stable) and their corresponding variable stars is minimum.

The pixel distance, differences of stellar magnitudes and colours of identified variables and their comparison stars are listed in the Table 6 and Table 4.

Difference values of pixel coordinated and colours of selected stable stars are conforming their non-usability for study of variable stars via differential photomety. However, comparative analysis of their light curves becomes a tool to understand the nature of instrumental errors and to trace the impact of pseudo-variability. In this background, the differential photometry has been performed for confirming the nature of variable stars above the 3σ limit of variation of instrumental errors of detected stars within DOLIDZE 14 and NGC 1960.

5.6 Nature of stellar light curves

The light curves of potential variable stars and their corresponding stable stars are depicted in **Figures 4 to 10(A)**. To distinguish the instrumental variations from stellar light curves, the stellar magnitudes are subtracted from each other and resulting curves are defined as comparative light curves. The author has applied the differential photometry over absolute photometry for constructing such comparative light curves. This process is defined as differential-absolute photometry and leads an effective reduction of the effects in comparative light curves due to sky conditions of observational night.

The light curves for each variable and its selected comparison stars (set of three stars) have shown in the different panels of these figures. In this connection, each set of stars have four panels. Top panel shows the light curve of potential variables and middle panels show the light curves of selected comparison stars. The fourth panel of each set have three lines of blue, red and black colour for representing the comparative light curves. The blue and red lines are shown the field subtracted light curves of variable through comparison stars, whereas black line represents the difference of stellar magnitudes of selected comparison stars. A constant spacing of comparative light curves is obtained for stable comparison stars, while the varied spacing of these curves confirms the signature of stellar variability. Since, obtained information of stellar variability

Table 4 Variable IDs for cluster are listed in first column . V-magnitudes of variable stars of NGC 1960 and I-magnitudes of variable stars of DOLIDZE 14 are given in second column. Values of colour, $(B-V)$, of variable stars of NGC 1960 and colour, $(J-K)$ of variable stars of DOLIDZE 14 are listed in third column. Fourth, fifth and sixth columns indicate the difference of magnitudes for potential variable and its comparison stars. Seventh, eighth and ninth columns represent delta differences of prescribed colour values. In case of NGC 1960, V-magnitudes are standard magnitude as reported by Joshi & Tyagi, 2015.

1:- DOLIDZE 14

Va. ID.	I-magnitude for Variable V	Colour (J-K) for Variable V	$\Delta_{I_{mag}}$ V & C1	$\Delta_{I_{mag}}$ V & C2	$\Delta_{I_{mag}}$ C1 & C2	$\Delta_{(J-K)}$ V & C1	$\Delta_{(J-K)}$ V & C2	$\Delta_{(J-K)}$ C1 & C2
V_1	13.784 ± 0.015	0.264 ± 0.038	-0.370	-0.483	-0.113	-0.394	-0.487	-0.093
V_2	17.385 ± 0.030	0.656 ± 0.072	0.013	0.011	-0.002	-0.206	-0.173	0.033
V_3	17.804 ± 0.055	0.139 ± 0.183	0.003	-0.006	-0.009	0.074	0.301	0.227
V_4	18.501 ± 0.086	0.595 ± 0.139	0.032	-0.001	-0.033	0.396	-0.133	-0.529

2:- NGC 1960

Va. ID.	V-magnitude for Variable V	Colour (B-V) for Variable V	$\Delta_{V_{mag}}$ V & C1	$\Delta_{V_{mag}}$ V & C2	$\Delta_{V_{mag}}$ C1 & C2	$\Delta_{(B-V)}$ V & C1	$\Delta_{(B-V)}$ V & C2	$\Delta_{(B-V)}$ C1 & C2
V_1	14.007 ± 0.004	0.511 ± 0.005	-0.032	-0.017	-0.015	-0.164	-0.078	0.086
V_2	14.020 ± 0.004	0.520 ± 0.007	0.029	0.044	-0.015	-0.415	-0.152	0.263
V_3	14.127 ± 0.005	0.991 ± 0.007	-0.040	-0.011	-0.029	0.418	0.438	0.020
V_4	14.215 ± 0.008	0.569 ± 0.008	-0.036	0.019	-0.022	-0.055	-0.145	-0.123
V_5	14.674 ± 0.006	0.674 ± 0.007	0.002	0.005	-0.003	-0.013	0.025	0.038
V_6	15.060 ± 0.004	0.743 ± 0.006	0.001	0.007	-0.007	-0.088	-0.269	-0.181
V_7	15.155 ± 0.009	1.522 ± 0.014	-0.001	0.004	-0.005	0.760	0.509	-0.251
V_8	15.345 ± 0.005	0.766 ± 0.005	-0.013	-0.008	-0.005	-0.920	0.072	0.992
V_9	15.497 ± 0.004	0.938 ± 0.005	-0.042	0.011	-0.053	-0.164	-1.216	-1.052
V_{10}	15.592 ± 0.004	0.778 ± 0.005	0.005	0.022	-0.017	-0.064	-0.027	0.037
V_{11}	15.668 ± 0.005	0.966 ± 0.007	-0.034	0.011	-0.045	0.326	-0.103	-0.429
V_{12}	15.711 ± 0.007	0.946 ± 0.009	0.089	0.091	0.012	0.135	-0.002	-0.123
V_{13}	15.769 ± 0.004	0.820 ± 0.006	-0.001	0.031	0.009	-0.364	-0.032	0.373
V_{14}	15.969 ± 0.004	0.944 ± 0.007	-0.017	0.001	-0.018	-0.669	-0.061	0.608
V_{15}	16.197 ± 0.005	0.809 ± 0.008	-0.002	0.016	-0.018	-0.387	-0.217	0.170
V_{16}	16.279 ± 0.006	0.984 ± 0.008	0.022	0.041	-0.019	-0.001	-0.709	-0.708
V_{17}	16.369 ± 0.007	1.070 ± 0.011	-0.007	0.022	-0.029	0.285	-0.840	-1.125
V_{18}	16.673 ± 0.007	1.112 ± 0.009	-0.007	0.006	-0.013	0.242	0.224	-0.018

Table 5 The first column shows variabe ID of variables within studied clusters. The second and third columns represent *RA* and *DEC* respectively. The values of period of detected variable stars are estimated through the PERIOD04 and PerSea Software as listed in fourth and seventh columns respectively.

1:- DOLIDZE 14

Variable ID	RA ($J2000$)	DEC ($J2000$)	Period (days) PERIOD04	Amplitude (mmag)	Power [PERIOD04]	Period (days) PerSea
V_1	4 : 07 : 12.11	27 : 15 : 17.7	0.0599±0.0067	270	04.356	0.0606±0.0068
V_2	4 : 06 : 56.99	27 : 13 : 13.4	0.0939±0.0195	474	03.051	0.0714±0.0074
V_3	4 : 07 : 02.32	27 : 24 : 27.8	0.1349±0.0359?	311	12.169	0.1428±0.0173?
V_4	4 : 06 : 21.87	27 : 26 : 01.5	0.0674±0.0085	327	07.793	0.0714±0.0062

2:- NGC 1960

Variable ID	RA ($J2000$)	DEC ($J2000$)	Period (days) PERIOD04	Amplitude (mmag)	Power [PERIOD04]	Period (days) PerSea
V_1	05 : 36 : 25.11	34 : 06 : 10.2	0.3057±0.0815	102	66.948	0.4000±0.1055
V_2	05 : 36 : 17.85	34 : 09 : 14.8	0.2246±0.0599	165	56.576	0.6250±0.0274
V_3	05 : 36 : 33.33	34 : 06 : 05.4	0.3598±0.0001	086	99.261	0.4000±0.2086
V_4	05 : 36 : 20.05	34 : 09 : 14.6	0.3115±0.1168	062	35.608	0.2857±0.0706
V_5	05 : 35 : 55.79	34 : 10 : 07.6	0.3182±0.0848	248	34.752	0.2857±0.0454 (2.4949 :^{*2})
V_6	05 : 36 : 28.54	34 : 09 : 05.8	0.1528±0.0194	069	24.174	0.1538±0.0369
V_7	05 : 35 : 53.49	34 : 08 : 09.6	0.1747±0.0254	065	23.504	0.1695±0.0154
V_8	05 : 36 : 21.20	34 : 05 : 25.4	0.2864±0.0007	073	65.225	0.2857±0.0947
V_9	05 : 36 : 17.96	34 : 05 : 38.7	0.2667±0.0006	095	48.289	0.4629±0.0.0399
V_{10}	05 : 36 : 39.17	34 : 11 : 42.8	0.1886±0.0003	074	31.753	0.2404±0.0226
V_{11}	05 : 36 : 17.84	34 : 06 : 31.8	1.1053±0.0007	124	185.267	1.098±0.1033
V_{12}	05 : 36 : 37.89	34 : 03 : 27.5	0.8538±0.0004	084	93.789	0.6667±1.0505
V_{13}	05 : 36 : 21.85	34 : 05 : 40.9	0.3057±0.0815	076	35.455	0.2857±0.0762
V_{14}	05 : 36 : 43.52	34 : 05 : 08.8	0.2665±0.0711	077	13.036	0.2222±0.0775
V_{15}	05 : 36 : 21.81	34 : 05 : 34.1	0.3039±0.0810	072	23.669	0.2041±0.0.0105
V_{16}	05 : 35 : 44.69	34 : 03 : 03.4	0.3005±0.0801	087	22.739	0.2941±0.0171
V_{17}	05 : 36 : 38.67	34 : 10 : 29.8	− − − −−	− − − −−	− − −	− − − −−
V_{18}	05 : 36 : 17.92	34 : 09 : 51.1	− − − −−	− − − −−	− − −	− − − −−

changes rapidly with the sky and weather conditions, therefore, we can not find stellar variability of the order of *mmag* during session of bright moon and observational nights, having fog and high humidity. As a result, we have selected smoother light curve to compute the period of identified variable after the visual inspection of individual light curve of each observational night. **The period values have determined by two different methodology as statistical and ANOVA analysis. The period values are not agreeing with each other in 6 cases (V_2, V_3, V_9, V_{10}, V_{12}, V_{15}) among variable stars within Field of View of NGC 1960. In the case of V_2, V_{10} and V_{12} of NGC 1960, both values are seems to be considerable for periodic analysis. It is impossible to determine the true period for variable star V_3 of NGC 1960 as the nightly data strings are about the same computed values.**

5.7 Comparative Analysis of SSM with essential conditions of Differential Photometry

The major characteristics of comparative light curves of present comparison stars of variable stars of NGC 1960 are obtained as below,
(1)- The shifted and varied magnitude differences are found in comparative light curves of comparison stars of variable stars V_1, V_2 and V_{12} .
(2)- A constant value of magnitude difference is found in comparative light curves of comparison stars of variable stars V_6, V_8 and V_{11} during observations of individual night. However, shifting of magnitude difference is altered night to night observations.
(3)- A constant value of magnitude differences is found in comparative light curves of comparison stars of variable V_3, V_4, V_9, V_{14} and V_{17} during the observations on date 24-01-2012, 11-12-2013 and 20-12-2013. Similarly, a shifted and constant value of magnitude differences is obtained in light curves of these stars during the observations on date 12-01-2015 and 08-02-2015.
(4)- A constant value of magnitude differences is found in comparative light curves of comparison stars of variable V_5, V_9, V_{10}, V_{13}, V_{15}, V_{16} and V_{18} during the observations.

Thus, detected variable stars of NGC 1960 are listed in four different groups as per comparative light curves of their comparison stars. After deep investigation of Table 6 and Table 4, we have not found any criteria of geometric distribution of comparison stars and their colour-difference values for separating variable stars of NGC 1960 into these obtained groups. It indicates that there are no need of comparison stars for any variable star after implication of SSM approach. In nutshell, the present SSM approach is seems to be reliable to evaluate the stellar variable nature within studied clusters.

6 Fourier Transform of variables and their Pulsations

The light curves of stars contain aliases frequencies due to the interaction of pulsation of variables and the noise or instrumental errors. Such summation of noise and pulsation signal of variable is removed through the utilization of comparison star during differentiate photometry and becomes an effective method to reduce the uncertainty of detected pulsation signal in the scattered data points of light curves of variables. After confirming the pulsation signal of stars, we need a periodogram to estimate the spectral density of a signal during the pulsation signal processing. Now days, the periodogram are computed from the stellar light curves through the implemented of algorithms such as LombScargle folding (Lomb 1976; Scargle 1982), Box-fitting Least Squares or "BLS" (Kovacs et al. 2002) and Plavchan (Plavchan et al. 2008). Standard and advanced Fourier transform techniques are useful in the analysis of astrophysical time series of very long duration (Ransom et al. 2002) due to their better computing ability. The Lomb-Scargle algorithm is a variation of the Discrete Fourier Transform (DFT), in which a time series is decomposed into a linear combination of sinusoidal functions[3]. This algorithm has been implemented by us to detect pulsation of variables and constructed the Fourier-Discrete-periodogram (FDP). In this connection, the 'PERIOD-04'[4] and 'PerSea'[5] software are utilized to estimate the period of new identified variable stars. 'Period04' is dedicated to the statistical analysis of large astronomical time series with gaps and offers tools to extract the individual frequencies from the multi-periodic content. Other hand, 'PerSea' is based on the analysis of variance (ANOVA) algorithm. In the Table 5, we listed the resultant estimated period of variables through the both software. The phase-folded diagrams of detected regular variables are constructed by utilizing the values of pulsation period as per 'Period04'. The phase-folded light curves of variables of DOLIDZE 14 have been depicted in the Figure 10(B), whereas these curves of variables of NGC 1960 are shown in the Figure 11(A). In these diagrams, the phase values of any variable at time t is defined to the decimal part of $(t - JD)/P$, where

[3] exoplanetarchive.ipac.caltech.edu/docs/pgram

[4] www.univie.ac.at/tops/Period04

[5] www.home.umk.pl/ gmac/SAVS/soft.html

Table 6 Variable IDs for cluster are listed in first column. Second, third and fourth columns indicate the **separation pixel-distances** for potential short periodic variable stars and its comparison stars.

1:- DOLIDZE 14

Variable ID	$\Delta\ D$ (in pixel)	$\Delta\ D$ (in pixel)	$\Delta\ D$ (in pixel)	SNR	Variable Type
V_1	830.818	540.589	294.191	18.00	*Miscellaneous*
V_2	235.701	808.347	682.126	15.80	*Rotational*
V_3	466.591	657.623	281.851	05.65	*Miscellaneous*
V_4	920.656	954.320	716.691	03.80	White Dwarfs

2:- NGC 1960

Variable ID	$\Delta\ D$ (in pixel)	$\Delta\ D$ (in pixel)	$\Delta\ D$ (in pixel)	SNR	Variable Type
V_1	234.715	373.093	262.214	25.50	*Miscellaneous*
V_2	189.041	509.045	596.828	41.25	$\gamma - Dor$
V_3	448.043	145.154	334.378	17.20	*Miscellaneous*
V_4	231.421	389.344	202.745	07.75	$\gamma - Dor$ (JO20)
V_5	483.260	158.671	444.375	41.33	EB?
V_6	339.534	659.349	792.740	17.25	*Ellipsoidal*
V_7	648.068	916.607	860.138	07.22	*Ellipsoidal*
V_8	145.462	373.379	261.138	14.60	*Rotational*
V_9	643.228	392.418	753.954	23.75	*RRC*
V_{10}	128.526	925.765	814.031	18.50	*LADS*
V_{11}	132.993	483.626	614.331	24.80	*EB*
V_{12}	445.491	756.433	312.356	12.00	*Rotational*
V_{13}	554.006	448.464	267.522	19.00	*Miscellaneous*
V_{14}	635.751	813.743	298.683	19.25	*Miscellaneous*
V_{15}	272.533	569.389	297.607	14.40	*LADS*
V_{16}	763.334	599.666	346.557	14.50	*Miscellaneous*
V_{17}	466.030	782.811	320.374	$----$	Irregular
V_{18}	291.715	398.561	640.928	$----$	Irregular

JD and P represent the Initial Julian Date and Period of the variables. In this connection, the value of JD is 2455951.11037 and 2456943.35851 for NGC 1960 and DOLIDZE 14 respectively.

6.1 Smoothness of phase diagrams and change in amplitude of pulsation

There is too much of a scattering of data points in the original phase diagrams to investigate and shape the nature of stellar variability. Such scattered data points in the curves are occurred due to instrumental errors and noise, due to which, it is not possible to accurately classify the nature of stellar variability. To overcome this problem, we adopt the average moving procedure for construction of these diagrams. In this procedure, data points are arranged in increasing order according to their phase values from 0 to 1. In this connection, the average values are determined for sets of five data points such as 1-5, 2-6, 3-7 and so on. This procedure is repeated until we are not computed the average of last remaining five data points. However, a sufficient fraction of the amplitude of light curve also decreases during adoption of this procedure. The resultant phase-folded curves of variables are found to be smooth in comparison of original diagrams. As a result, we conclude that amplitude of stellar pulsation decreases with the increment of smoothness of the phase-folded diagram of variables due to the moving average procedure. In the Figures 10(B) and 11(A), the phase diagrams of variables constructed through the resultant data points as per the average moving procedure. **The signal-to-noise ratio (SNR) is defined as $SNR = \frac{A}{e_A}$, where A and e_A are amplitude of light curve and mean estimation error in stellar magnitude respectively. SNR values of variable stars are listed in Table 6.**

7 Mean proper Motion and Membership Analysis

7.1 Mean Proper Motion of Core region of NGC 1960

The proper motion study of this cluster was carried out by Meurers (1958), Chian & Zhu (1966) Sanner et al. (2000) and Joshi et al. (2020) [JO20 now onward]. We compared our catalogue with Gaia EDR3 data given by Gaia collaboration et al. (2016, 2021) and found 1579 common stars between them within the studied core region. The distribution of these stars in μ_x-μ_y plane is shown in Fig. **??**. The dark filled circles in the figure are those stars that were used to determine the mean proper-motion of the cluster NGC 1960. These stars were identified after excluding those stars which lie outside 3σ deviation from the mean value of proper motion in both RA and DEC directions. After 3σ iteration processes, we have found 1405 stars from which we obtained following mean proper motion in RA and DEC direction of the cluster NGC 1960.

$$\bar{\mu_x},\ \bar{\mu_y} = 0.314 \pm 0.026\, mas/yr,\ -2.333 \pm 0.037\, mas/yr$$

JO20 has been estimated the mean proper motion of whole cluster of NGC 1960 in RA and DEC directions as -0.143 ± 0.008 $mas\ yr^{-1}$ and -3.395 ± 0.008 respectively. **Since, JO20 shows a very different selection of cluster members which does not include stars centered around zero pm, therefore their different proper motion values are obvious due to the selection of stars, the applied methodology. Due to the inclusion of field stars,** the standard deviation values ($\sigma_\alpha,\ \sigma_\delta$) of stellar proper motions of NGC 1960 are found to be 0.996 and 1.402 in RA and DEC respectively. Using these values, the resultant standard deviation $\sigma = \sqrt{\sigma_\alpha^2 + \sigma_\delta^2}$ is estimated as 1.734. **This standard deviations of the stellar proper motion of cluster NGC 1960 are not compatible with the standard errors of present work as well as the work of JO20.** Thus, the different values of proper motions of both studies indicates that the stellar members of this cluster may segregated in inner and outer regions according their proper motion values.

7.2 Mean Proper Motion of DOLIDZE 14

In the case of DOLIDZE 14, a total of 1137 stars is found within periphery of radius 9.8 $arcmin$ at GAIA database. We are found proper motions for 887 stars among them, which are used for computation of mean proper motion of DOLIDZE 14. After 3σ iteration processes, we have found 761 stars from which we obtained following mean proper motion in RA and DEC direction of the cluster DOLIDZE 14.

$$\bar{\mu_x},\ \bar{\mu_y} = 1.050 \pm 0.083\, mas/yr,\ -2.254 \pm 0.093\, mas/yr$$

Due to the inclusion of field stars, the estimated standard deviation values ($\sigma_\alpha,\ \sigma_\delta$) of proper motion values of stars of DOLIDZE 14 are 2.288 and 2.601 in RA and DEC respectively. These values give resultant standard deviation $\sigma = \sqrt{\sigma_\alpha^2 + \sigma_\delta^2}$ as 3.465. **These values are not compatible with the standard errors of the stellar proper motion of DOLIDZE 14 and confirms the proper decontamination process of filed stars from cluster region.**

7.3 Kinematic Probabilities

In the present analysis, those stars are consider to be kinematic members for each cluster, which lie within 3σ limit of the mean proper motion of studied cluster. The proper motion probability is assigned to be 1 for stars having coincident proper motions with the cluster, whereas the proper motion probability is assigned to be 0 for stars having proper motions outside the 3σ limit (Joshi, G.C. 2022). **By utilizing extracted stellar proper motion from GAIA EDR3 database**, new kinematic probabilities of stellar members of each cluster is computed as $P_{pm} = 1 - \frac{\sqrt{(\mu_\alpha - \bar{\mu_\alpha})^2 + (\mu_\delta - \bar{\mu_\delta})^2}}{3\sigma}$. These values of variable stars of both clusters are listed in sixth column of **Table 7**.

7.4 Stellar Parallax and Membership

The individual stellar distance of each potential variable star is computed by using the parallax information as extracted from GAIA EDR3 database and listed in third column of Table 7. These values are compared with the estimated distance for concerned cluster via CMD analysis. Positional membership of cluster is assigned for those variable stars, whom distance is equal to that of its parent cluster and no positional membership is assigned for other variable stars. The comparative detail of kinematic and positional probabilities for each individual variable stars in Sections 9 & 10.

8 Comparative study of cluster's parameters with variable stars

8.1 Variable Stars and ZAMS of NGC 1960

By using $(U-B)$ vs $(B-V)$ Two colour Diagram (TCD), Joshi & Tyagi (2015a) has been determined reddening, $E(B-V) = 0.23\pm0.02$ mag. JO20 has also computed the reddening, 0.24 ± 0.02 mag, which is close to previous one. In the present work, the location of variable stars of NGC 1960 has been depicted in $(U-B)$ vs $(B-V)$ TCD along-with Zero-Age-Main-Sequence (ZAMS) as shown in Figure 16. A ZAMS star has its minimum radius, its maximum mass (for single star evolution), its bluest colour (or hottest effective temperature), and its central core possesses its peak H/He (Hanson 1998). After deep inspection of TCD and GAIA database for cluster, author has been drawn following facts:
(1)- Variable stars V_1, V_2, V_3. V_4 are found to be ZAMS stars and have close brightness to each other in V-band. The locations of V_1, V_2 and V_4 at the near of bump in $(U-B)$ vs $(B-V)$ TCD, whereas the location of V_3 is found to be far away these stars. This facts leads different class of V_3.
(2)- Variable stars V_8, V_{12}, V_{13}, V_{14} and V_{16} are belong to ZAMS of cluster. Variable stars V_8 and V_{12} are member of cluster 1960 and may poses the character of same class of variable stars. Variable stars V_{13}, V_{14} and V_{16} are field stars leads a fact that field stars are also located in just main sequence of cluster.
(3)- Variable stars V_6, V_{10}, V_{11}, V_{15}, V_{17} and V_{18} are not belong to main sequence of cluster and have a confirm membership of cluster.
(4)- Variable stars V_5, V_7, and V_9 neither belong to main sequence of cluster nor have a member of cluster.

8.2 CMDs analysis for NGC 1960

The log-age of this cluster is reported by Kharchenko et al. (2004), Joshi & Tyagi (2015a) and JO20 as 7.62 (yr), 7.35 (yr) and 7.44 (yr), respectively. Joshi & Tyagi (2015a) shown the most probable members (MPMs) in $(B-V)$ vs V Colour Magnitude Diagram (CMD) by comprehensive analysis of photometric, kinematic and spatial probabilistic criteria. These MPMs are found along with MS of NGC 1960 and also well aligned with a well fitted theoretical isochrone as depicted in upper panels of Figure 17. The pink line of each CMD represents the well fitted theoretical as computed by Joshi & Tyagi (2015a). In the $(J-H)$ vs H CMD, author did not find stellar alignment by MPMs along with theoretical isochrone for H-magnitude range of 12.5-13.2 mag as shown in Figure 17(B). It leads a correction in an estimation of distance-modulus. Author overplot Marigo's theoretical isochrones on the CMDs by varying the distance modulus and age simultaneously by keeping reddening $E(B-V) = 0.23$ mag. From the best visual isochrone fit to the varying age and distance combinations, author obtained a distance modulus $(V-M_V) = 11.05\pm0.0.30$ mag and $log(Age) = 7.35\pm0.05$ (yr) for cluster NGC 1960. Employing the correction for the reddening and assuming a normal reddening law, this corresponds to a true distance modulus $(m-M)_0 = 10.34\pm0.30$ mag or a distance of 1.169 ± 0.173 kpc for the cluster. **This distance is close to that of** 1.17 ± 0.06 kpc as estimated by JO20 via a mean parallax, 0.86 ± 0.05 mas, for probable cluster members of NGC 1960 (For this purpose, parallax values were extracted by JO20 from GAIA database). The computed value of distance modulus is utilized to identify the true member of cluster as per retrieved value of distance/parallax value of individual star.

The best fitted theoretical isochrones in each CMD is represented by black line and identified variable stars

Table 7 Prallax and distance values of studied variable stars are listed in second and third columns respectively. The stelar proper motion values of R.A. and DEC deirection are given in fourth and fifth columns respectively. The estimated kinematic probabilities of variables are listed in sixth column.

1:- DOLIDZE 14

Variable ID	Parallax (mas)	Distance (kpc)	Proper Motion in RA (δ)	Proper Motion in DEC (μ)	kinematic Pro. (Old)	kinematic Pro. (GAIA)
V_1	1.2234±0.0162	0.817±0.011	2.317±0.019	−7.763±0.012	−−	0.456
V_2	0.7388±0.0772	1.354±0.141	1.903±0.094	1.060±0.054	−−	0.671
V_3	0.2453±0.0709	4.077±1.178	0.590±0.077	−0.856±0.046	−−	0.858
V_4	0.9287±0.1791	1.077±0.208	−1.934±0.204	−3.928±0.116	−−	0.671

2:- NGC 1960

Variable ID	Parallax (mas)	Distance (kpc)	Proper Motion in RA (δ)	Proper Motion in DEC (μ)	kinematic Pro. (Old)	kinematic Pro. (GAIA)
V_1	0.8858±0.0188	1.129±0.024	−0.204±0.023	−3.406±0.016	0.40	0.771
V_2	0.8430±0.0180	1.186±0.025	−0.011±0.023	−3.506±0.017	0.35	0.766
V_3	2.9243±0.0228	0.342±0.003	−3.018±0.027	−4.932±0.019	0.06	0.188
V_4	0.8382±0.0194	1.193±0.027	−0.432±0.024	−3.219±0.017	0.99	0.777
V_5	0.2889±0.0255	3.461±0.305	0.675±0.028	−2.292±0.021	0.05	0.930
V_6	0.8543±0.0254	1.171±0.035	−0.209±0.034	−3.440±0.023	0.81	0.765
V_7	0.1985±0.0275	5.038±0.698	0.113±0.027	−1.594±0.021	0.00	0.853
V_8	0.8206±0.0350	1.219±0.052	−0.042±0.040	−3.525±0.026	0.79	0.761
V_9	0.4966±0.0857	2.014±0.348	0.010±0.097	−3.579±0.072	0.91	0.753
V_{10}	0.8022±0.0309	1.246±0.048	−0.244±0.036	−3.276±0.027	0.04	0.789
V_{11}	0.8130±0.0350	1.230±0.053	−0.401±0.043	−3.543±0.030	0.94	0.730
V_{12}	0.9063±0.0400	1.103±0.049	−0.059±0.049	−3.355±0.035	0.00	0.791
V_{13}	0.4407±0.0366	2.269±0.188	0.723±0.041	−3.327±0.029	0.00	0.793
V_{14}	0.0995±0.1441	10.050±14.555	0.692±0.159	−2.518±0.128	0.99	0.919
V_{15}	0.9037±0.0496	1.106±0.061	−0.331±0.055	−3.593±0.037	0.00	0.728
V_{16}	1.1574±0.0478	0.864±0.036	4.521±0.057	−1.697±0.038	0.93	0.182
V_{17}	0.9037±0.0448	1.107±0.055	−0.178±0.055	−3.418±0.040	0.52	0.771
V_{18}	0.8396±0.0460	1.191±0.065	−0.246±0.054	−3.425±0.039	0.95	0.764

are depicted by red dots. Variable stars V_3 and V_7 shows colour excess in near-infrared bands, however these stars also found along-with the theoretical isochrone in $W_2 - W_1$ *vs* W_1 CMD as depicted in Figure 17(C).

8.3 Range of Instability strip in the case of NGC 1960

The instability strip is a narrow, almost vertical region in HR diagram, which contains many different type of variable stars. Most stars more massive than Sun enter the instability and become variable at least once after they have left the main sequence (MS) [6]. This strip intersect the MS in the region of A and F stars (have mass 1-2 $M_{\odot}$) of studied clusters and extends to G and early K bright super-giants. The common area of instability strip and MS of OCL NGC 1960 seems to be important region (includes A and F stars) to understand the cluster dynamics through the stellar variability and vice-versa. **To determine the location of the A/F type stars in the colour-magnitude diagram, distance modulus,** $(V - M_V) = 11.05\pm0.30$ *mag*, **was applied to obtain the V-magnitudes.** In this connection, the upper and lower limit of region, have A and F stars, are found to be 13.17±0.30 *mag* of $V - band$ and 16.61±0.30 *mag* of $V - band$, respectively and prescribed intercepted region also least affected by the brighter stars and their neighbourhood. As a result, author is carried out time series analysis for finding stellar variability within this magnitude-range. A total of eighteen variables of NGC 1960 are identified in this magnitude-range. **In the present case of NGC 1960. author did not perform any analysis to search variable stars in near the turn-off region and fainter stellar region.**

8.4 CMDs analysis for DOLIDZE 14

In the case of DOLIDZE 14, there are no saturated brighter star of unresolved center. As a result, author did not need employ any selection criteria of stellar magnitudes to identify variable stars for this cluster. The red dots of lower panels of Figure 17 represent identified variable stars for DOLIDZE 14. The distance modulus and distance for cluster DOLIDZE 14 has been estimated by Joshi et al. (2015) as 11.12±0.18 *mag* and 1.67±0.14 *kpc* respectively. In this connection, the best fitted isochrone is depicted by black solid line in Figure 17, whereas pink and blue lines represent lower and upper limits for apparent distance modulus. The distance of identified variable stars of this cluster are listed in table 7. Variable star V_2 is close to cluster periphery, whereas variable star V_4 seems to be confirmed member of cluster. Other two variable stars V_1 and V_3 are not belong to cluster as per known parameters.

[6] astronomy.swin.edu.au/cosmos/I/Instability Strips

9 Detected Variables in DOLIDZE 14

The time series observation of this cluster has been taken in Near-Infrared region by using I-band with effective wavelength 8000 $\mathring{A}$. In the present analysis, a total of 4 variable stars are found in the observed field of DOLIDZE 14.

9.1 Miscellaneous type variable star

Some periodic stars could not be classified in any particular class of variable stars as per their estimated parameters and phased light curves.

9.1.1 Star IDs 004 (V_1), 005 and 006 of DOLIDZE 14

As par 'PERIOD04' and 'PerSea' code analysis, the period values of V_1 are found to be 0.0599±0.0067 d and 0.0606±0.0068 respectively. Its individual distance value (0.817±0.011) is very far away from the cluster distance. Its least kinematic probabilistic value also supports that it is not a member of cluster. Thus, it can not be classified as a main sequence star for the studied cluster. Potential variable V_1 is located just near the turn off point of CMD with blue colour. As per analysis of properties of this star, it seems to be a miscellaneous type variable star.
Light curve of this variable has been compared with the light curves of star IDs 005 ($4^h : 06^m : 26.85^s$, $+27^0 : 18^{'} : 24.2^{"}$) and 006 ($4^h : 06^m : 43.39^s$, $+27^0 : 17^{'} : 46.9^{"}$). Light curves of selected comparison stars do not show any sign of periodic variability.

9.1.2 Star IDs 109, 110 (V_3) and 111 of DOLIDZE 14

Variable star V_3 poses a **a single minima** in its light curve. This feature leads **its potential candidature as a variable star.** The computed period is 0.1349±0.0359 d **and** 0.1428±0.0173 d **as per codes 'PEROD04' and 'PerSea' respectively. Both values are approximate similar with length of data string during** observation session for DOLIDZE 14 and leads a dubious analysis for **assign classification of its stellar variability. Thus, it is quite impossible to derive a period from a single-night light curve that extent for a few hours, with only a single event of s drop in the light curve**. Its distance is found to be 4.077±1.178 *kpc* and leads it is as

a non-member of cluster. As a result, variable star V_3 may be a system of binary stars with unknown periodic eclipse.
Light curves of comparison star IDs 109 ($4^h : 06^m : 42.69^s$, $+27^0 : 20^{'} : 30.2^{"}$) and 111 ($4^h : 06^m : 45.90^s$, $+27^0 : 17^{'} : 00.8^{"}$) have no sign of stellar variability as depicted in Figure 10.

9.2 Potential Rotational Variable star

Rotational variable stars have a change in apparent brightness due to large spots on their surfaces. The light curves of such type variable stars are typically very noisy due to evolution of star spots over time.

9.2.1 Star IDs 085, 086 and 088 (V_2) of DOLIDZE 14

A value of period for variable star V_2 has been calculated to be 0.0939±0.0195 d and 0.0714±0.0074 by the code of 'PERIOD04' and 'PerSea' respectively. Its amplitude, distance and kinematic membership for cluster is computed to be 0.088 mag, 1.354±0.141 kpc and 0.671 respectively. Its location in $(J-H)$ vs H CMD has found towards red colour as depicted in Figure 17. As a result, this star seems similar to a rotational type star. As DOLIDZE 14 is an old cluster having an age of about 1.26±0.08 Gyr, it is rare/ impossible that any star in the cluster are found to be rotational variables. In this connection, this variable star can not have a member of cluster.
In Figure 10, the comparative Light curves of star IDs 085 ($4^h : 07^m : 02.90^s$, $+27^0 : 15^{'} : 53.4^{"}$) and 086 ($4^h : 06^m : 38.14^s$, $+27^0 : 22^{'} : 33.0^{"}$) along with variable star V_2 has been depicted. Author did not find any sign of periodic variability in the light curves of said comparison stars.

9.3 Potential Binary system of stars

A sudden drop in brightness of binary system finds due to eclipse and transit of its component stars during their orbit along plane of our line of sight.

9.3.1 Star IDs 183, 184(V_4) and 185 of DOLIDZE 14

Variable star V_4 is not found to be a member of of DOLIDZE 14 as per its distance 1.077±0.208 kpc and membership probability 0.671. By using the codes of 'PERIOD04' and 'PerSea', the period of this variable star is computed as 0.0674±0.0085 d and 0.0714±0.0062 d respectively. **The orbital periods of binary stars do not get as shorts as** 0.1 $days$ **unless the components are white dwarfs or similar compact objects**. Thus, light curve of variable star V_4 poses character of **white dwarfs** as depicted in Figure 10.
Light curves of comparison star IDs 183 ($4^h : 06^m : 24.45^s$, $+27^0 : 14^{'} : 24.9^{"}$) and 185 ($4^h : 07^m : 02.11^s$, $+27^0 : 17^{'} : 52.8^{"}$) are shown the more variation in brightness compare with other comparison stars of studied cluster. However, there are no periodic variation in comparative light curve of comparison stars (Star IDs 183 and 185) and have low variation of brightness compare to their comparative light curves with variable star V_4.

10 Detected Variables in NGC 1960

In this paper, eighteen variables were detected in the observed field of NGC 1960, among them only four variable stars are common with JO20. According to the behavior of the light curves and the period analysis, classification of detected variables were made. Among the eighteen detected variables of NGC 1960, one as EB, one as planet transit, one as $\gamma - Dor$, two as $\delta\ Scuti - \gamma - Dor$, two as LADS, two as irregular, two as rotational, three as RRC and four as Ellipsoidal type variable stars.

10.1 $\gamma - Doradus$ variables

The light curves of regular variables are repeating with a constant value of time (i.e. its period). A multi-periodic stars with g-mode pulsation is known to be $\gamma - Doradus$. These are typically young, early F- or late A-type main stars with periods in the range of about $0.3 - 3$ d and brightness fluctuation ~ 0.1 mag Balona et al. (2011).

10.1.1 Star ID 606 (V_2), 616 and 626 of NGC 1960)

In the case of variable star ID 606, star IDs 616 ($5^h : 36^m : 26.45^s$, $+34^0 : 07^{'} : 39.3^{"}$) and ID 624 ($5^h : 35^m : 50.83^s$, $+34^0 : 06^{'} : 03.6^{"}$) are selected for comparing their light curves with it. JO20 is assigned ID 606 as cluster member $\delta - Scuti$ variable star with period 0.27632±0.00008 d and it is denoted by V_{35} in their analysis. In the present work, its period is computed by the code of 'PERIOD04' and 'PerSea' as 0.2246±0.0599 d and 0.6250±0.0274 d, respectively. **Since, both computed vales are far away from the length of data string, therefore it has a characteristic of multi-periodicity.** Since its light curves in Figure 4 are not showing any indication of period value below 7.6 hours, therefore its period value via Anova analysis is seems to be more accurate. Thus,

Star ID 606 is found to be $\gamma - Doradus$ variable star instead of $\delta - Scuti$. Its kinematic probability makes it as most probabilistic member of cluster.

The light curves of ID 616 are showing irregular flux variations, whereas light curves of ID 624 have a characteristics of long periodic variables. Almost constant magnitude found for ID 624 during 7-8 hours observations.

10.2 RR Lyre stars

Over 80 % of all variables known in globular clusters are RR Lyre stars (Clement et al. 2001). One d-type RR Lyre variable star in the open cluster NGC 2141 has been reported by Luo (2015). RR Lyrae variables do not follow a strict period-luminosity relationship at visual wavelengths, although they do in the infrared K-band (Catelan et al. 2004).

10.2.1 Star IDs 1431, 1470 (V_9) and 1484 of NGC 1960

The variable star V_9 is assigned to be rotational variable star, main sequence star and cluster member by JO20 and marked by V_{48} in their analysis. Its period is computed to be 0.2667±0.0006 d and 0.4629±0.0399 d by code of 'PERIOD04' and 'PerSea' respectively. These codes clearly provide two distinct values of period. **It seems that computed period** 0.2667±0.0006 d **(as per 'PERIOD04' code)is the a average length of data strings in 2013 and 2015, whereas period value** 0.4629±0.0399 d **(as per 'PerSea' code) is cross matched with period** 0.47483±0.00023 **as estimated by JO20.** Its location in $(U-B)$ vs $(V-B)$ TCD indicates that it does not fulfill the criteria of ZAMS within errors as depicted in Figure 16. Its distance is 2.014±0.348 kpc as per GAIA database, which is very far away from the cluster NGC1960. Thus, variable star V_9 neither main sequence star nor a member of cluster NGC 1960. Its highest probabilistic values are just coincidence with members of cluster. Since, its characteristics are not well matched with rotational type variable star, therefore author switched off its previous classification as did by JO20.
The slowly descending and quick ascending nature of its phase-folded curve indicate that variable star V_9 is a RR Lyre star.
Star IDs 1431 ($5^h:36^m:45.65^s,\ +34^0:11^{'}:25.0^{''}$) and 1484 ($5^h:36^m:00.93^s,\ +34^0:09^{'}:07.7^{''}$) has selected comparison stars for variable star v_9. Their locations in 13 and 12 are marked by C1(V9) and C2(V9) respectively. As per visual inspection, author found these comparison stars are far away from the variable star V_9. The comparative light curves of star IDs 1431 and ID 1484 show a constant magnitude difference during entire observational session. As per GAIA database, The parallax value for Star Ids 1431 and 1484 is 0.6473 mas and 0.2435 mas, respectively. The colour-difference $(B-V)_0$ for both comparison stars is greater than 1.0 mag. Such pair of comparison stars is not possible for any given variable star as per differential photomery. As a result, magnitude variation of stars is free from stellar distance and colour-difference in absolute/ standard photometry. However, author found some amount of magnitude variation for both comparison stars, but it is seems to be impact of instrumental nature due to their constant magnitude difference.

10.3 Eclipsing Binaries type Variable Stars

Eclipsing binaries are easily classified into two main groups: detached system or semidetached (Balona et al. 2015). Spherical or slightly ellipsoidal components are found in detached system (Algol type, EA), whereas tidally distorted stars are present in semidetached system (β Lyre System, EB). The light remains almost constant between eclipses of EA systems. Between eclipses, a continuous change of the combined brightness is found for EB system, leads impossibility to specify the exact times of onset and end of eclipses. Stars with planets may also show flux variations if associated planets for any star pass between Earth and the star.

10.3.1 Star IDs 900 (V_5), 902 and 904 of NGC 1960

Star ID 902 is marked by V_{55} by JO20 and it is assigned to be field star in their analysis. In addition, they found a minima in its phase curve with amplitude of 218 $mmag$. **In the case of** $V_5(ID900)$ **at figure 5, the different light curve show a partial eclipse and part of an eclipse. The full eclipse is detected in its light curve of 20 December 2013 and a portion of eclipse also detected in its light curve of 12 January 2015. The gap of both detected eclipses is 01 year 23 days 3 hours. The other nights show a constant data string. This is a classical light curve of an eclipsing binary due the rounded shape.** Author also found only one full minima in its light curves **with amplitude of** 248 $mmag$ **and it is close to estimated amplitude by JO20**. In the present work, the light curves of variable star V_5 are depicted in Figure 5. The time of eclipse is computed to be 0.3182±0.0848 d and 0.2857±0.0454 d through the codes of 'PERIOD04' and 'PerSea' respectively, which are not true periods. These both values are equivalent to those data strings, in which eclipse has detected. After visual inspection of light curves of this variable, estimated time of

eclipse is approximately 0.216±0.018 *d*. Its distance is 3.461±0.305 *kpc* and far away from the cluster periphery. Thus, it is a background field star in the field of cluster NGC 1960.
Light curves of Star IDs 902 ($5^h : 36^m : 25.02^s$, $34^o : 09^{'} : 17.5^{''}$) and 904 ($5^h : 35^m : 58.41^s$, $34^o : 08^{'} : 11.8^{''}$) are selected for comparative analysis with variable star V_9. Both comparison stars have nearby colour, $((B-V)_0)$, value with variable star V_9. Light curves of Star ID 904 contain the short periodic variation with low amplitude, whereas light curves of star ID 2 have irregular variation of brightness. Since, their comparative light curves have almost constant value of brightness fluctuation, therefore, fluctuation of their light curves is a result of instrumental errors in nature.

10.3.2 Star IDs 1576, 1601 (V_{11}), 1613 of NGC 1960

Based on 'PERIOD04' and 'PerSea' code analysis, author obtained period value for V_{11} as 1.1053±0.0007 *d* and 1.0980±0.1033 *d*, respectively. Its distance is 1.230±0.053 *kpc* from us and its kinematic probability of membership in cluster is estimated to be 0.73 as per GAIA database. Thus, variable star V_{11} is a member of cluster. It is easily seen in its light curves, which are depicted in Figure 7 that short periodic variations are superimposed with its principal period. It becomes difficult to specify exact time of onset and end of eclipses of companion stars due to their continuous change of brightness and its phase-folded diagram shows superimposed character of both eclipses as depicted in Figure 11. As a result, this star is classified as semidetached eclipsing binary (EB) type variable star.
The pattern of brightness variation in light curves for star ID 1576 ($5^h : 36^m : 23.38^s$, $34^o : 05^{'} : 18.1^{''}$) is similar to variable star V_{11} as depicted in Figure 7. As a result, author concludes that star ID 1576 is also a EB star with low amplitude. During the observational session of each night, light curves of star ID 1613 ($5^h : 36^m : 02.64^s$, $34^o : 11^{'} : 46.0^{''}$) shows incremental slop over time with less inclination. In this connection, the fluctuation of its light curves is seems to be instrumental errors in nature.

10.4 Ellipsoidal Variable stars

In the periodogram of an ellipsoidal binary, sharp peaks are found at the fundamental frequency and its harmonics. Usually only the first harmonic is visible and the amplitude of fundamental frequency is less than first harmonic in some cases. As a consequence of differences in harmonic content, the shapes of the light curves can be very different (Balona et al. 2015). These stars are close binary system and tidally distorted components. There are no eclipses in these variables due to the low inclination of the orbital axis, but the changing aspect towards us causes a change in brightness. Such brightness variation are a combination of tidal distortion, reflection and beaming. The period of the reflection and beaming contributions is the same as the orbital period whereas the ellipsoidal effect has half the orbital period (Balona et al. 2015).

10.4.1 Star IDs 1123 (V_6), 1124 and 1130 of NGC 1960

Based on the codes of 'PERIOD04' and 'PerSea', the period of V_6 is found to be 0.1528±0.0194 *d* and 0.1538±0.0369 *d*, respectively. Its distance (1.171±0.035 *kpc*) and kinematic probabilistic value (0.765) indicate that it is a member of cluster. Since, non-sinusoidal variation is found in its phase folded light curve, therefore it contains character of ellipsoidal type variable star. However, comprehensive analysis of its light curves during whole observational session indicates that it is an irregular type variable. As a result, it is classified as an irregular variable with character of ellipsoidal.
Star ID 1124 ($5^h : 36^m : 28.92^s$, $34^o : 13^{'} : 23.2^{''}$) is selected as first comparison star for variable star V_6. It shows almost constant magnitude over time as shown in Figure 5. Thus, it is classified as standard star in the direction of cluster NGC 1960 and its physical location is marked by C1(V6) in Figure 12.
Similarly, star ID 1130 ($5^h : 35^m : 48.78^s$, $34^o : 07^{'} : 46.3^{''}$) is selected as second comparison star for variable star V_6. This star is classified as irregular type variable by JO20 and marked by V_{70} in their analysis. After visual inspection of its light curves in Figure 5, author also confirms its character of irregular type variable star.

10.4.2 Star ID 1197, 1199 (V_7), 1204 of NGC 1960

The value of period for variable star V_7 is computed to be 0.1747±0.0254 *d* and 0.1695±0.0154 *d* by using codes of 'PERIOD04' and 'PerSea' respectively. In the present work, its kinematic probabilistic value is estimated to be 0.853 as per GAIA database. Unfortunately, its distance (5.038±0.698 *kpc*) does not confirm its membership for a member of cluster. Due to a non-sinusoidal variation of brightness in its light curves, variable star V_7 is classified as ellipsoidal type variable. Its position in $(U-B)$ vs $(B-V)$ TCD confirms its redden character.
Its First Comparison star, ID 1197 ($5^h : 36^m : 25.21^s$, $34^o : 13^{'} : 04.1^{''}$), shows constant magnitude

during observational session as depicted in Figure 6. As a result, it is a standard star and its position is marked by C1(V7) in Figure 12.
Similarly, light curves of its second comparison star, ID 1204 ($5^h : 36^m : 43.20^s$, $34^o : 02^{'} : 51.6^{''}$), show the character of irregular type variable.

10.5 Rotational Variable

Stellar rotation and magnetic activity are normally associated with a main-sequence star of G or later spectral type (Joshi et al. 2020). Amplitude of pulsation of these stars have typically less than 0.1 mag. Thus, these stars are characterized by small amplitude, and red in colour $(B-V)_0 > 0.5\ mag$. Periods of rotational variable stars can widely vary due to its tied with the rotation of the stars themselves.

10.5.1 Star IDs 1345, 1348 and 1350 (V_8) of NGC 1960

By Using codes of 'PERIOD04' and 'PerSea', the value of period for V_8 is estimated to be 0.2864±0.0007 d and 0.2857±0.0947 d respectively. **The length of individual data strings is** 0.3167 d **and** 0.3000 d **on date 20/12/2013 and 12/01/2015, respectively and these values are greater than** 0.2864±0.0007 d**. Its character of variability is confirmed in individual data strings.** It is located at 1.219±0.052 kpc from us and this value is close with the distance of cluster. In this connection, its kinematic probabilistic value for cluster membership is 0.761 leads a member of studied cluster. It is red in colour, $(B-V)_0 = 0.766\ mag$. Its location in $(U-B)$ vs $(B-V)$ TCD is found along with ZAMS as depicted in Figure 16. All the above characters make it a rotational type variable star.
Light curves of star IDs 1348 ($5^h : 36^m : 29.70^s$, $34^o : 04^{'} : 53.6^{''}$) and 1345 ($5^h : 36^m : 43.22^s$, $34^o : 06^{'} : 38.6^{''}$) are depicted in Figure 6. Almost constant magnitude in light curves of star ID 138 make it a standard star, whereas star ID 1345 contains a character of long periodic type variable stars.

10.5.2 Star IDs 1644 (V_{12}), 1732 and 1734 of NGC 1960

Based on 'PERIOD04' and 'PerSea' code analysis, obtained value of period for variable star V_{12} is 0.8538±0.0004 d and 0.6667±1.0505 respectively. In $(U-B)$ vs $(B-V)$ TCD, it is just located on the main sequence. It contains redden character in colour, $(B-V)_0 = 0.946\ mag$. As per GAIA database, its distance is found to be 1.103±0.049 kpc with kinematic probability 0.791. Thus, it is a member of studied cluster with main sequence. Amplitude of this variable is found to be 94 $mmag$ via code of PERIOD04. In this connection, it is classified as rotational type variable star.
Light curves of star ID 1732 ($5^h : 36^m : 44.29^s$, $34^o : 08^{'} : 55.9^{''}$) shows short term variability with low amplitude, which seems to be instrumental error in nature. Beside this, it is approximately constant magnitude during observation. Other hand, Light curves of star ID 1734 ($5^h : 36^m : 46.46^s$, $34^o : 12^{'} : 51.3^{''}$) show a incremental slop of low inclination over observation as depicted in Figure 7.

10.6 Low Amplitude Delta Scuti Variable

Low-amplitude delta Scuti stars (LADS) contains pulsation with smaller amplitudes. The low-amplitude stars can be pre-main, main or post-main sequence stars, and may either be multiperiodic or monoperiodic [7].

10.6.1 Star IDs 1549 (V_{10}), 1553 and 1569 of NGC 1960

The value of distance (1.246±0.048 kpc) and kinematic probability (0.789) of variable star V_{10} confirms its membership of the cluster. Its location in $(U-B)$ vs $(B-V)$ TCD makes it as a post-main sequence star. Author analyzed the frequencies of variable star V_{10} with Fourier and variance analysis by using codes of 'PERIOD04' and 'PerSea'. After these analyses, the computed period is found to be $P_1 = 0.1886\pm0.0003$ and $P_2 = 0.2404\pm0.0226$, respectively, leads $P_1/P_2 = 0.78$. Amplitude of pulsation is 74 $mmmag$ as per Lomb-Scargle algorithm. So it is suggested that V_{10} is a multi-periodic $\delta - Scuti$ star with low amplitude.
Due to almost constant difference of stellar magnitudes in comparative light curves of Star IDs 1553 ($5^h : 36^m : 34.70^s$, $34^o : 10^{'} : 22.7^{''}$) and 1569 ($5^h : 35^m : 49.15^s$, $34^o : 06^{'} : 15.1^{''}$), their magnitude variation for an observational night is a result of instrumental transformation. However, light curves of star ID 1569 show a character of long-term variability as shown in Figure 7.

10.6.2 Star IDs 2195, 2198 (V_{15}) and 2222 of NGC 1960

The variable star (V_{15}) is a member of cluster due to its distance (1.106±0.061 kpc) and kinematic probability

[7] $aavso.org/vsots_delsct$

(0.728). It is also found a post-main sequence star as its position in $(U-B)$ vs $(B-V)$ TCD. The value of period for variable star V_{15} is computed to be 0.3039±0.0810 d and 0.2041±0.0105 d by using the codes of 'PERIOD04' and 'PerSea' respectively. **Since, computed value of** 0.3039±0.0810 d **(as per PERIOD04) is close to length of individual data string therefore, it is not a true period for variable star** V_{15}**.** However, it leads to ratio of $\nu_1 : \nu_2 = 3 : 2$. As per Lomb-Scargle algorithm, pulsation amplitude is 72 $mmag$ for this star. Thus, it is seems to be low amplitude $\delta - Scuti$ variable star.

There are no sign of reasonable variability in the light curves of star IDs 2195 ($5^h : 36^m : 08.50^s$, $34^o : 07^{'} : 37.9^{''}$) and 2222 ($5^h : 35^m : 55.14^s$, $34^o : 10^{'} : 10.8^{''}$) and their comparative light curves show almost constant difference for their magnitudes as depicted in Figure 8.

10.7 Irregular and miscellaneous Variable Stars

Mira variables have less regular light curves with large amplitudes of several magnitudes, while semi-regular variables are less regular with the smaller amplitudes (Samus et al. 2017). In this connection, amplitudes of light curves of irregular variables does not occur after a fixed time interval and shape of their light curves have found in an uncertain pattern. As a result, the variations in brightness show no regular periodicity in an irregular type variable star. Such stars are divided into eruptive and irregular pulsating variable stars. The variation of brightness of an eruptive variable star happens due to violent processes and flares occurring in its chromosphere ana coronae. Eruptive variable stars are found near the main sequence.

10.7.1 Star IDs 635, 645 and 649 (V_3) of NGC 1960

The codes of 'PERIOD04' and 'PerSea' provide its period value as 0.3598±0.0001 d and 0.4000±0.2086 d respectively. **These values are close to length of individual data strings in 2015. The length of data string (**0.3598±0.0001 d**) of variable star** V_3 **leads** a peculiar phase-fold diagram with slowly descending and quick ascending branches as similar to the *RR Lyre* variable stars. In this connection, its least kinematic probabilistic value and distance indicate that it is not a member of cluster NGC 1960. However, its position in $(B-V)$ *vs* V CMD and $(U-B)$ *vs* $(V-B)$ TCD is just on the main sequence. Its position in $(U-B)$ *vs* $(V-B)$ TCD is found to be far away from the group of identified $\delta - Scuti$ variable stars. In addition, **length of individual data strings** is too long for normal δ *Scuti* star. In these circumstance, it is impossible to classify its variability type. **As a result, it is listed as miscellaneous variable star in present analysis.**

In the case of this variable star, Star IDs 635 ($5^h : 36^m : 09.47^s$, $+34^0 : 08^{'} : 51.2^{''}$) and 645 ($5^h : 36^m : 29.11^s$, $+34^0 : 07^{'} : 42.2^{''}$) are selected for the comparative analysis. Star ID 635 is assigned to be $\gamma - Dor$ variable star by JO20. In this connection, author found that light curves of Star ID 635 shows characteristic similarities that of star ID 624. Similarly, light curves of star IDs 616 and 645 have similar characteristics. Thus, the nature of light curves of star IDs 616, 624, 635 and 645 is either uncertain in nature or some kind of irregular variability.

10.7.2 Star IDs 1701, 1702 (V_{13}) and 1732 of NGC 1960

A value of distance for variable star, V_{13}, is 2.269±0.188 kpc as per GAIA database. Its kinematic probabilistic value shows just coincide with the member of cluster. Its light curves shows a non-sinusoidal variation of brightness as depicted in Figure 8. As per codes of 'PERIOD04' and 'PerSea', the estimated value of period for variable star V_{13} is 0.3057±0.0815 d and 0.2857±0.0762 d, respectively. **Both values are similar to time length of individual data string during 2015 leads an misleading period. Phase curve via** 0.3057±0.0815 d **poses a fine phase curve as shown in Figure 11 for ID 1702. It period is seem to be coincidentally closer with length of data string**. As a result, computed It is classified as **miscellaneous** type variable star **due to lack of continuous data**.

Star IDs 1701 ($5^h : 36^m : 36.95^s$, $34^o : 11^{'} : 57.0^{''}$) and 1732 ($5^h : 36^m : 44.29^s$, $34^o : 08^{'} : 55.9^{''}$) are selected for comparative analysis and their positions are marked by C1(V13) and C2(V13) in Figure 13. After visual inspection of light curves of both comparison stars in Figure 8, author found a constant magnitude difference for both comparison stars. As a result, it is concluded that character of irregular type variable of both stars is an instrumental effect in nature.

10.7.3 Star IDs 1893, 1914 (V_{14}) and 1915 of NGC 1960

As per codes of 'PERIOD04' and 'PerSea', estimated value of period for variable star V_{14} is computed to be 0.2665±0.0711 d and 0.2222±0.0775 d, respectively. **Both compuated values are similar to average length of data strings.** It is located 10.050±14.555 kpc as per GAIA database, which is highly uncertain. Only highly kinematic probabilistic

value does not enough to assign membership status for any stars. Its location in $(U-B)$ vs $(B-V)$ TCD is just on the main sequence. Its depicted light curves in Figure 8 show a non-sinusoidal variation of brightness. **The pixel coordinates and light curves of this variable star suggested that its flux is influenced by side effects leads an uncertainty for computing periods as well as analysis of its light curve. As a result, it is classified as miscellaneous** type variable star.
Star IDs 1893 ($5^h:36^m:13.78^s,\ 34^o:10^{'}:18.2^{''}$) and 1915 ($5^h:36^m:18.07^s,\ 34^o:13^{'}:58.4^{''}$) in Figure 13 are marked by C1(V14) and C2(V14) respectively. Light curves of Star ID 1893 show character of long periodic variables, whereas Light curves of star ID 1915 are almost constant for some night of observation and have incremental slope with low inclination for other nights of observation.

10.7.4 Star IDs 2323 (V_{16}), 2352 and 2379 of NGC 1960

As per the codes of 'PERIOD04' and 'PerSea', the estimated values of period for V_{16} are 0.3005±0.0801 d and 0.2941±0.0171 d respectively. Its phase curve via 0.3005±0.0801 d posses a character of asymmetrical magnitude variation with increasing rapidly and decreasing slowly. The said phase curve **is seems to be distorted in nature as** depicted in Figure 11. **Both periodic found to be closer to length of individual data-string in 2015, therefore both are not true period. Such misleading period produced distortion in phase diagram compare to their light curve.** Its distance has given to be 0.864±0.036 *kpc* in GAIA database and it is close to us with respect to the cluster NGC 1960. In this connection, its least kinematic probabilistic value (as per GAIA database) also confirms it as Field Star. Although, its position in $(U-B)$ *vs* $(V-B)$ TCD is just on the main sequence as depicted in Figure 16.
Author has selected two stars, ID 2352 ($5^h:36^m:03.82^s,\ +34^0:11^{'}:51.5^{''}$) and ID 2379 ($5^h:36^m:12.86^s,\ +34^0:07^{'}:54.1^{''}$), for comparing their light curves with that of variable star V_{16}. Both stars are showing approximate constant magnitude difference during entire observation sessions. However, their light curves have character of Long Periodic Variables, but seems to be instrumental effect. As per observations of each individual night, they have low magnitude variation compare to variable star V_{16} as depicted in upper panels of Figure 9. The pixel distances of these stars (IDs 2323, 2352, 2379) indicate that they are far away to each other **as listed in Table 6**. Colour, $(B-V)_o$, values of V_{16} and ID 2352 are close to each other, but far away from that of ID 2379. Thus, similar character of light curves for ID 2352 and ID 2379 confirms colour- free selection of comparison stars during time series analysis via absolute photometry.

10.7.5 Star IDs 2439, 2451 (V_{17}) and 2479 of NGC 1960

The values of distance and kinematic probability for variable star V_{17} are found to be 1.107±0.055 *kpc* and 0.771 respectively. As a result, it is assigned as a member of cluster and find near the main sequence as shown in Figure 16. Author did not find any sign of regular pulsation for it. A speck of stellar brightness for this variable star has detected on date 11 December 2013 as depicted in Figure 9. The period of this variable star can not be computed by the codes of 'PERIOD04' and 'PerSea'. Thus, this variable star is suggested to be an irregular type variable.
In the case of variable star V_{17}, the comparison stars are ID 2439 ($5^h:36^m:14.60^s,\ 34^o:07^{'}:21.1^{''}$) and ID 2479 ($5^h:35^m:56.35^s,\ 34^o:05^{'}:53.3^{''}$). The comparative light curves of both comparison stars has almost constant difference of brightness during observation of each night. Comparative light curves of V_{17} with its comparison stars indicate that spacing of light curves are varying night to night as depicted in the middle Set of Panels of Figure 9. It may be due to character of long variability of V_{17} with irregular pulsation. In addition, the light curves of star ID 2439 also show a character of long term variability.

10.7.6 Star IDs 2868, 2875 (V_{18}) and 2889 of NGC 1960

The variable star V_{18} is a cluster member due to its kinematic probability (0.764) of membership and distance (1.191±0.065 *kpc*). Light curves of variable star V_{18} do not show any sign of periodic pulsation. As per observation on date on date 11 December 2013, flare type structure is detected in the constructed light curve of this variable star. Its location find near the main sequence in $(U-B)$ vs $(B-V)$ TCD and depicted in Figure 16. The codes of 'PERIOD04' and 'PerSea' do not enable to compute period for this variable star. As a result, it is classified as irregular variable star with eruptive phenomena.
In the case of V_{18}, the comparison stars are ID 2868 ($5^h:36^m:34.54^s,\ 34^o:08^{'}:31.6^{''}$) and ID 2889 ($5^h:35^m:55.53^s,\ 34^o:07^{'}:52.2^{''}$). Due to the almost constant brightness in the light curves for star ID 2868,

it is assigned as the standard star. The black comparative light curve of filed stars does not show any noticeable fluctuation in flux, whereas, comparative light curves of V_{18} variable and filed stars confirm the long term stellar variability of V_{18} as depicted in the lower set of panels of Figure 9.

10.8 Characteristics test of $\delta - Scuti - \gamma - Doradus$ hybrid variables

Generally, $\gamma - Doradus$ instability strip is found to be below the $\delta - Scuti$ strip. Several authors reported that some portion of instability strips of both these classes is overlap to each other. Such hybrid candidates are already discovered in open clusters by Hartman et al. (2008) and Joshi et al. (2020). **The estimated log(age) of cluster NGC 1960 is** $7.35\pm0.05\ yr$**, similar to J20. This concerns a young open cluster in which the A/F-type stars are not evolved.** $\delta - Sct$ **stars tend to have high pulsation mode frequencies (**$\nu \geq 35\ d^{-1}$**) as inferred from theoretical models Michel et al. (2017). Such fast variability should be detectable in the light curves, except for the fact that the amplitudes tend to be very small.**

10.8.1 Star IDs 592, 595 and 600 (V_1) of NGC 1960

Author has selected two stars, ID 592 ($5^h : 36^m : 39.44^s,\ +34^0 : 06^{'} : 12.3^{''}$) and ID 595 ($5^h : 36^m : 41.27^s,\ +34^0 : 09^{'} : 29.9^{''}$), for comparing their light curves with Star ID 600 and these stars are marked by C1(V1) and C2(V2) in Figure 13. Joshi et al. (2020) has assigned ID 595 as a cluster member and a hybrid δ *Scuti* γ *Daradus* variable star and it is marked by V_{27} in their analysis. All of these stars have minimum in V-magnitude and colour (B-V) as listed in Table 5. After inspection of light curves of Star IDs 592 and 595 in Figure 4, author noted that both stars have shown approximate similar pattern. The light curves of ID 595 have regular pattern of flux variation with very low amplitude and author considered it as an effect of instrumental pseudo-variability. **Thus, it is impossible to find character of young** $\delta - Scuti$ **stars based on low quality data sets.** Light curves of star ID 600 have shown prominent variation in its magnitude. The value of its period is found to be $0.3057\pm0.0815\ d$ and $0.4000\pm0.1055\ d$ by code of 'PERIOD04' and 'PerSea', respectively. **These value are similar to data strings. As a result, author did not advocated about its true period**. It has characteristics similar to variable star V_4 star and it is listed as miscellaneous in present analysis. Its location within cluster is shown in Figure 2 by mark M36(V1). It is also found more kinematic probabilistic member of cluster by the author.

10.8.2 Star IDs 678, 688 (V_4) and 694 of NGC 1960)

Star IDs 678 ($5^h : 36^m : 33.38^s,\ +34^0 : 10^{'} : 13.0^{''}$) and 694 ($5^h : 36^m : 37.21^s,\ +34^0 : 12^{'} : 39.3^{''}$) are selected as possible comparison star. These stars are marked by C1(V1) and C2(V2) in Figure 13 and their physical coordinates are found closest compare than other set of stars. Variable star V_4 is assigned to be a γ *Daradus* variable star with period 1.07066 d and marked by V_{62} in the work of Joshi et al. (2020). In the present analysis, its period is found to be $0.3115\pm0.1168\ d$ by the code of 'PERIOD04', whereas the said value is 0.2857 ± 0.0706 by the ANOVA analysis as per code of 'PerSea'. **These values are closed to average length of data strings.** It is more kinematic probabilistic member of cluster and marked by M36(V4) in Figure 2. In present study, author did not classify it due to circumstances of data.

The trend of light curves of Star IDs 678 and 694 are approximately similar to each other. However, light curves of star ID 694 shows a regular feature of short periodic variability and it is considered to be pseudo-variability by author.

11 Results and Discussion

The contamination of fluxes of fainter stars is occurred due to their nearby brighter stars. Author also found very high scatter data points in the light curves of brighter stars of NGC 1960 due to their **saturation** in the present deep photometric observations. As a result, author did not analysis the time series observations of brighter and their nearby stars.

Star IDs 1124, 1197, 1348 and 2868 of M36 have approximately constant stellar magnitude during whole observations, their celestial coordinates are ($5^h : 36^m : 28.92^s,\ 34^o : 13^{'} : 23.2^{''}$), ($5^h : 36^m : 25.21^s,\ 34^o : 13^{'} : 04.1^{''}$), ($5^h : 36^m : 29.70^s,\ 34^o : 04^{'} : 53.6^{''}$) and ($5^h : 36^m : 34.54^s,\ 34^o : 08^{'} : 31.6^{''}$) respectively. Thus, these stars are classified as the **constant** stars within cluster. As per GAIA database, the distance of stars 1124, 1197, 1348 and 2868 has been computed as $1.166\pm0.035\ kpc$, $1.152\pm0.036\ kpc$, $3.461\pm0.278\ kpc$ and $1.419\pm0.109\ kpc$ respectively. Thus, star IDs 1124 and 1197 are members of cluster NGC 1960.

Some variable stars (as V_2**) have two distinct period values via two distinct algorithm (ANOVA and statistical analysis). In the case**

of variable star V_2, statistical analysis computed a period value as found near to length of individual data strings in 2015, therefore it is not suitable for considering a true period. As a result, true period for variable star V_2 is 0.6250 ± 0.0274 d **as per ANOVA analysis.**

Among the 18 detected variable stars, only four are cross matched with JO20, whereas three of the 36 selected comparison stars are cross matched with JO20, whom stellar variability has not been confirmed in the present analysis. Thus, we concluded that the time series data of one night may leads an over-estimation of short periodic variables via absolute/standard phtotmetry. Since computed value of period for variable star V_3 of cluster DO14 is found to be nearly equal to time duration of its observation, therefore author did not classify this star as per period.

JO20 has used continuous time series data less than 3.5 hours for each observational night, whereas author has additional time series data of 5.4, 7.6, 7.2 and 5.6 hours as observed on dated 11-12-2013, 20-12-2013, 12-01-2015 and 08-02-2015 respectively. Since period value of variable star V_2 of M36 by JO20 is seems to be inaccurate in the view of additional data, therefore it is avoided to classify those variable stars, that have approximately same/ slightly longer period than the time duration of observation for a particular night.

In the case of DO14, author has constructed light curves for selected comparison stars by magnitude translation of non-standardized field via SSM approach, whereas light curves for selected comparison stars of M36 has constructed by absolute photometry via SSM approach. Their comparative analysis indicate that absolute photometry is a meaningful to search for variable stars in the target filed. SSM approach has given same trends of pseudo-variability for comparison stars in the field of both cluster. As a result, this approach confirms that resulting light curves of comparison stars do not depend on the nature of reference catalogue produced by either standard or instrumental magnitudes of stars.

Author concludes that the detection process of short-period variability from a single night nothing to do with the absolute/standard photometry. Although, the the appearance of a unique feature in light curves of potential variable star is confirmed through the differential photometry of similar stars.

12 Conclusion

The present analysis is dedicated to find the short periodic variable stars, having period less than 1 day. In this connection, author did not present any analysis for the classification of potential candidate of variable stars with the character of long periodic and irregular variability. To find small periodic variables, time series data for DOLIDZE 14 and NGC 1960 have been collected over one and five nights of observations, respectively. In this connection, the stellar light curves for NGC 1960 and DOLIDZE 14 are extracted from these time series data.

By deep investigate of stellar light curves, a total of 18 and 4 variable stars have been identified in the field of view of cluster NGC 1960 and DOLIDZE 14 respectively. Four of these 18 variable stars are cross matched with JO20. In addition, other three variable stars of JO20 are not found short pulsation stars in present analysis. To carry out the membership analysis for variable stars, the mean proper motion of NGC 1960 and DOLIDZE 14 in their RA and DEC directions were estimated as (0.314 ± 0.026 $mass/yr$ and -2.333 ± 0.037 $mass/yr$) and (1.050 ± 0.083 $mass/yr$ and -2.254 ± 0.093 $mass/yr$), respectively.

The time duration (1.2 yr) looks good for precise determination of Period of any variable star. As per 10 cases out of 18 for NGC 1960 (V_1, V_3, V_4, V_5, V_8, V_9, V_{13}, V_{14}, V_{15} and V_{16}), most derived periods are length of 0.25-0.30 days, this is the average length of the individual data strings in 2013 and 2015. This makes the period determination very suspicious. Thus, the large gap in between the nights (almost 1 yr) causes additional aliases. As a result, author concludes that it is impossible to determine the true periods, and the physical reason of the light variability based on such scare data sets poorly dispersed over a long period of time.

Due to the observational limitations of CCD camera of 1.04 m telescope at ARIES, a telescope equipped with a very high-capacity CCD camera is needed to carry out the task of searching for sign of variability in the brighter stars of NGC 1960.

13 Competing interest

The authors declare that they have no competing interest.

14 Consent for publication

Not applicable.

15 Ethics approval and Consent to participate

Not applicable.

Acknowdege

GCJ acknowledges the web-portal services of SIMBAD, VIZIER and ESO. Collection and observation of time series data of both clusters (NGC 1960 and DOLIDZE 14) performed by GCJ during 18 September 2012 to 27 April 2015. Director, ARIES gave permission to GCJ to use ARIES Data for research work via letter no. AO/2018/41 on date 12 April 2018.

References

Alter, G., Balazs, B., Ruprecht, J., Akademiai Kiada, Budapest, P. 3086, 2^{nd} edition (1970). VizieR online Data Catalog, VII/5A.

Balona, L. A., Guzik, J. A., Uytterhoeven, K., Smith, J. C., Tenenbaum, P., Twicken, J. D., The Kepler view of γ Doradus stars, MNRAS, **415**, 3531 (2011)

Balona, L. A., Baran, A. S., Daszynska-Daszkiewicz, J., De Cat, P., Analysis of *Kepler* B stars: rotational modulation and Maia variables, MNRAS, **451**, 1445 (2015)

Barkhatova K. A., Zokharova P. E., Shaskina L. P. & Oreknova L. K., Some Kinematic parameters of open cluster systems, Astron. Zh., **62**, 854 (1985)

Catelan, M., Pritzl, B. J., Smith, H. A., The RR Lyre Period-Luminosity Relation. I. Theoretical Calibration, The Astrophysical Journal Supplement Series, **154(2)**, 633 (2004)

Cantat-Gaudin T., & Anders, F., Clusters and Mirages: cataloguing stellar aggregates in the Milky Way, Astronomy and Astrophysics, **633**, A99 (2020)

Chian B. & Zhu G., An Investigation on the Proper-Motions of the Open Clusters NGC 1960, NGC 6530 and NGC 7380, Annals of the Shesan Section of the Shanghai Observatory, **26**, 53 (1966)

Clement, C. M., Muzzin, A., Dufton, Q., Ponnampalam, T., Wang, J., Burford, J., Richardson, A., Rosebery, T., Rowe, J. and Hogg, H. S., Variable stars in Galactic Globular Clusters, The Astronomical Journal, **122**, 2587 (2001)

Conrad, C., Scholz R.-D., Kharchenko, N. V. et al. A RAVE investigation on Galactic open clusters. II. Open cluster pairs, groups and complexes, Astronomy and Astrophysics, **600**, A106 (2017)

Delgado, A. J., Alfaro, E. J., Garrido, R., Garcia-Pelayo, J. M., Search for B-Type variables stars in open clusters, Information Bullatine on Variable Stars(IBVS), **2603**, 1 (1984)

Dias W. S., Monteiro H., Caetano, T. C., Lepine, J.R.D., Assafin, M. Oliveira A. F., Proper motions of the optically visible open clusters based on the UCAC4 catalog, Astronomy and Astrophysics, **564**, A79 (2014)

Dupret, M. A., Grigahcene, A., Garrido, R., Gabriel, M., Scuflaire, R., Theoretical instability strips for δ Scuti and γ Doradus syars, A&A, **414(2)**, L17 (2004)

Gaia collaboration et al., A&A, **595**, A2 (2016)

Gaia collaboration et al., A&A, **649**, A1 (2021)

Hanson, M.M., ZAMS O Stars, (Boulder-Munich II: Properties of Hot, Luminous Stars, Edited by Ian) ASP Conference Series 1998, 131-1.

Hartman, J.D., Gaudi, B.S., Holman, M.J., McLeod, B.A., Stanek, K.Z., Barranco, J.A., Pinsonneault, M.H., Kalirai, J.S., Deep MMT Transit Survey of the Open Cluster M37. II. Variable Stars., The Astrophysical Journal, **675**, 1254 (2008)

Hasan P., Kilambi G. C. & Hasan S. N., Near Infrared Photometry of the Young star clusters NGC 1960, NGC 2453 and NGC 2384, Bull. Astr. Soc. India, **33**, 151 (2005)

Hippke M., Learned J. G., Zee A., Edmondson W. H., Lindner J. F., Kia B., Ditto W. L., and Stevens I. R., Pulsation period variations in the RRc Lyrae star KIC 5520878, ApJ, **798**, 42 (2015)

Jeffries, R. D., Naylor, T., Mayne, N. J., Bell, C. P. M. and Littlefair, S. P., A lithium depletion boundary age of 22 Myr for NGC 1960, MNRAS, **434(3)**, 2438 (2013)

Johnson H. L. & Morgan W. W., Fundamental stellar photometry for standards of spectral type on the Revised System of the Yerkes Spectral Atlas, Astrophysical Journal, **117**, 313 (1953)

Joshi, Gireesh C., Dynamic Properties and Search of Variable Stars: NGC 1960, In: Mishra, G.C. editor. National Conference on Innovative Research in Chemical, Physical, Mathematical Sciences, Applied Statistics and Environment Dynamics (CPMSED-2015), Krishi Sanskriti Publications (New Delhi) ISBN: 978-93-85822-07-0; 2015, p. 22-27.

Joshi, Gireesh C.,Implication of Phase-folded Diagrams for Validation of the Nature of Stellar Variability I: the case of NGC 6866, Bulgarian Astronomical Journal, **37**, 01 (2022)

Joshi, Gireesh C. & Tyagi, R. K., Statistical analysis for precise estimation of Structural Properties of NGC 1960, Mathematical Sciences Int Research Journal, **4**, 384 (2015)

Joshi, Gireesh C. & Tyagi, R. K., Dynamical Features of Open Star Clusters: DOLIDZ 14, In: Mishra, G.C. editor. International Conference on Recent Trends in Applied Physical, Chemical Sciences, Mathematical/Statistical and Environmental Dynamics (PCME-2015) (ISNB: 978-81-930585-8-9), 2015, p. 37-42.

Joshi, Gireesh C., Joshi,Y. C., Joshi, S., Tyagi, R. K., Basic Parameters of open star clusters DILIDZE 14 and NGC 110 in infrared bands, New Astronomy, **40**, 68 (2015)

Joshi,Y. C., Joshi, S., Kumar,B., Mondal, S., Balona, L. A., MNRAS, **419**, 2379 (2012).

Joshi, Y. C., Maurya, J., John, A. A., Panchal, A., Joshi, S. and Kumar, B., Photometric, Kinematic and Variability study in the young open cluster NGC 1960, MNRAS, **492**, 3602 (2020)

Kharchenko N. V., Piskunov A. E., Roeser S., Schilbach E. & Schola R.-D., Astrophysical supplements to the ASCC-2.5 II. Membership probabilities in 520 Galactic open cluster sky areas, Astron. Nachr., **325**, 740 (2004)

Kovacs, G., Zucker, S., Mazeh, T., A box-fitting algorithm in the search for periodic transits, A&A, **391**, 369 (2002)

Landolt A. U., AJ, **104**, 340 (1992)

Lata S., Yadav R. K., Pandey A. K., Richichi A., Eswaraiah C., Kumar B., Kappelmann N. and Sharma S., Main-sequence variable stars in Young open cluster NGC 1893, MNRAS, **442(1)**, 273 (2014)

Lomb, N., Least-squares frequency analysis of unequally spaced data, AP&SS, **39(2)**, 447 (1976)

Luo, Y. P., Variable stars in the open cluster NGC 2141, RAA, **15(5)**, 733 (2015)

Luo Y. P., Zhang X. B., Deng L. C., and Han Z. W., Discovery of 14 new slowly pulsating b stars in the open cluster NGC 7654, ApJ Letters, **746**, L7 (2012)

Meurers J., Ein Stern-Aggregat im M 36. Mit 7 Textabbildungen, Z Astrophysics, **44**, 203 (1958)

Michel E., Dupret M.A., Reese D. et al., What CoroT tells us about $\delta-Scuti$ stars-Existence of a regular pattern and seismic indicates to characterize stars, EPJ Web Conferences, **160**, 03001 (2017)

Nilakshi, Sagar R., Pandey A. K. & Mohan V., A study of spacial structure of galactic open star clusters, A&A, **383**, 153 (2002)

Plavchan, P., Jura, M., Kirkpatrick, J. D., Cutri, R. M., Gallagher, S. C., Near-Infrared Variability in the 2MASS Calibration Fields: A search for planetary transit candidates, The Astronomical Journal Supplement Series, **175**, 191 (2008)

Ransom, S. M., Eikenberry, S. S., & Middleditch, J., Fourier Techniques for Very Long Astrophysical time-series analysis, AJ, **124**, 1788 (2002)

Samus, N. N., Kazarovets, E. V., Durlevich, O. V., Kireeva, N. N., Pastukhova, E. N., General catalogue of variable stars: Version GCVS 5.1, Astronomy Reports, **61**, 80 (2017)

Sanner, J., Altmann, M., Brunzendorf, J., Geffert, M., Photometric and kinematic studies of open star clusters. II. NGC 1960 (M 36) and NGC 2194, A&A, **357**, 471 (2000)

Sariya, D. P., Lata, S., Yadav, R. K. S., Variable stars in the globular cluster NGC 4590 (M 68), New Astronomy, **27**, 56 (2014)

Scargle, J. D., Studies in astronomical time series analysis. II. Statistical aspects of spectral analysis of unevenly spaced data, ApJ, **263**, 835 (1982)

Skrutskie, M. F., Cutri, R. M., Stiening, R., et al., The Two Micron All Sky Survey (2MASS), AJ, **131**, 1163 (2006)

Sharma S., Pandey A. K., Ogura K., Mito H., Tarusawa K. & Sager R., Wide-field CCD photometry around nine open clusters, AJ, **132**, 1669 (2006)

Sharma S., Pandey A. K., Ogura K., Aoki T., Pandey K., Sandhu T. S. & Sager R., Mass functions and photometric binaries in nine open clusters, AJ, **135**, 1934 (2008)

Smith, R., Jeffries, R. D., Dust discs around intermediate-mass and Sun-like stars in the 16 Myr old NGC 1960 open cluster, MNRAS, **420(4)**, 2884 (2012)

Stetson P. B., DAOPHOT: A Computer Program for Crowded-Field Stellar Photometry, PASP, **99**, 191 (1987)

Stetson P. B., 1992 in ASP conf. Ser. vol. 25, Astronomical Data Analysis Software and System, I. Astron. Soc. Pac., ed. Warrall D. M., and Biemesderfer C., Barnes J., San Francisco, 297

Wood, P. R. and Sebo, K. M., On the pulsation mode of Mira variables: evidence from the Large Magellanic cloud, MNRAS, **282(3)**, 958 (1996)

Wright E. L., Eisenhardt P. R. M., Mainzer A. K., et al., The Wide-field Infrared Survey Explorer (WISE): Mission Description and Initial On-orbit Performance, AJ, **140**, 1868 (2010)

This manuscript was prepared with the AAS LaTeX macros v5.2.

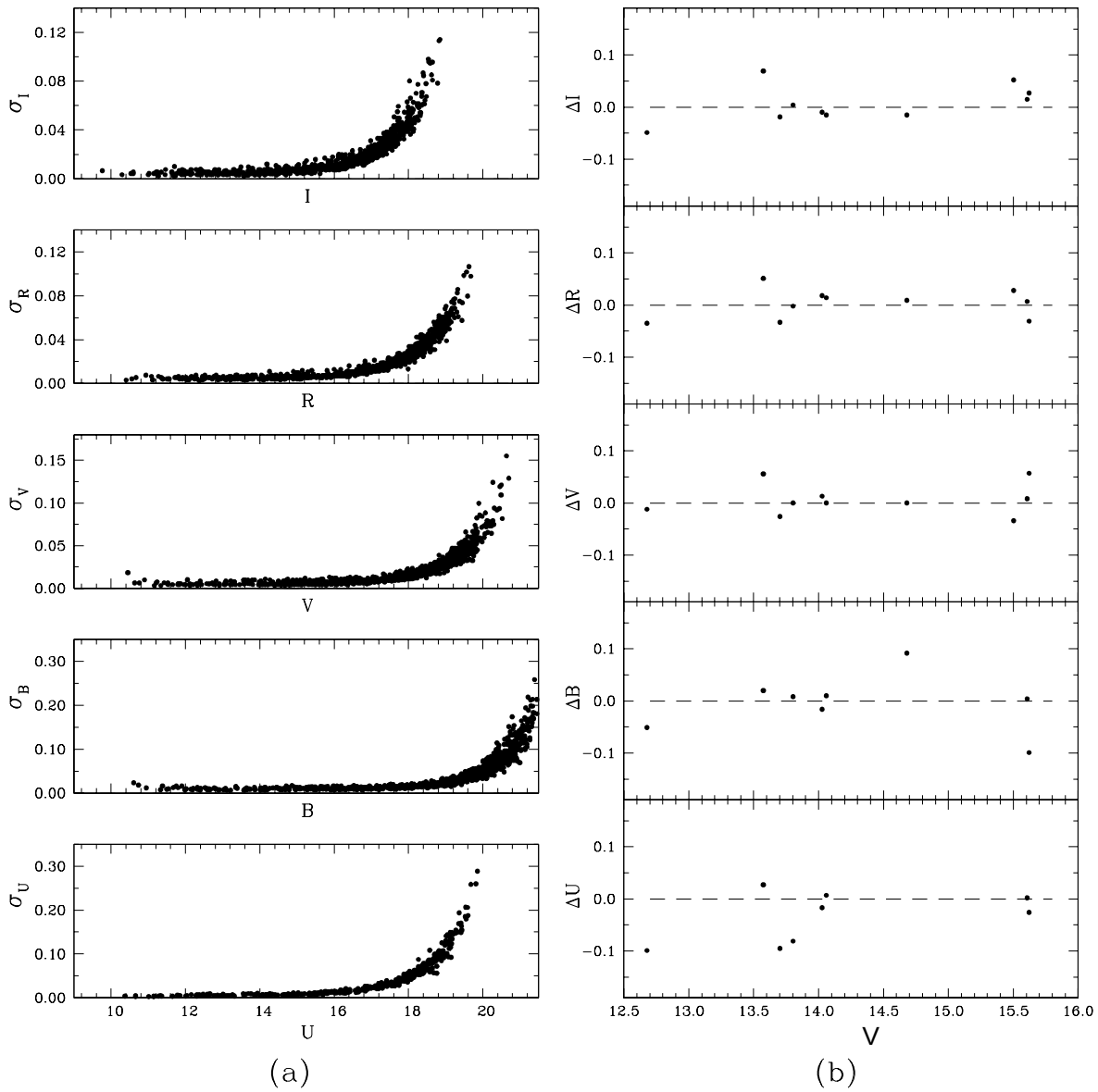

Fig. 3 In left panels, we present standard deviation (errors) of stars as a function of brightness. The right panels show difference between our estimated magnitudes with that of the Landolt's magnitude for the standard stars in $UBVRI$ passbands. The black dashed line represents zero shift.

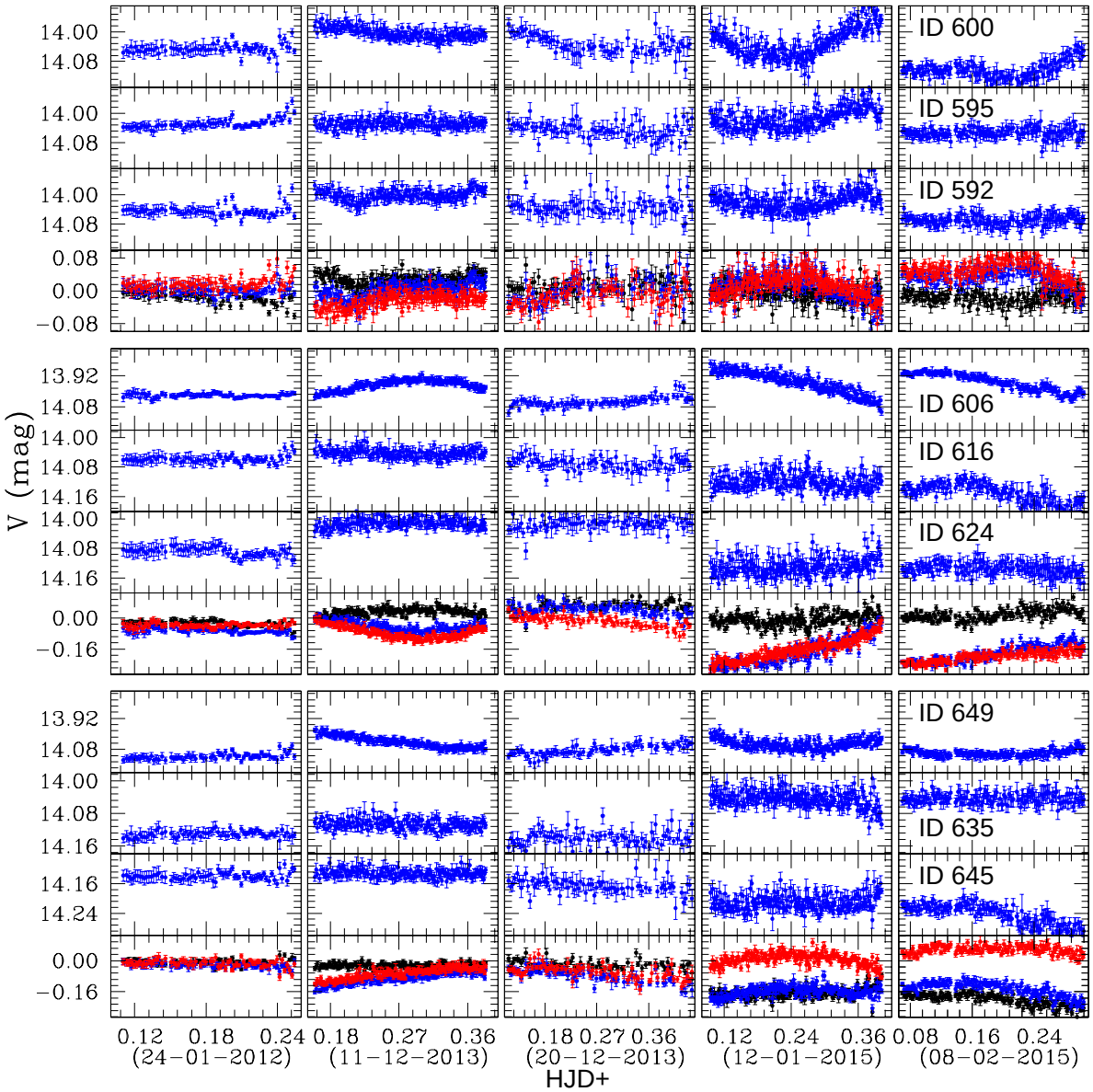

Fig. 4 The panels represent the stellar light curves for star IDs 592, 595, 600, 606, 616, 624, 635, 645 and 649 of cluster NGC 1960. The star IDs 592 and 595 are selected comparison stars for Potential variable (V_1, Star ID 600). The star IDs 616 and 624 are selected comparison stars for Potential variable (V_2, Star ID 606). The star IDs 635 and 645 are selected comparison stars for Potential variable (V_3, Star ID 649).

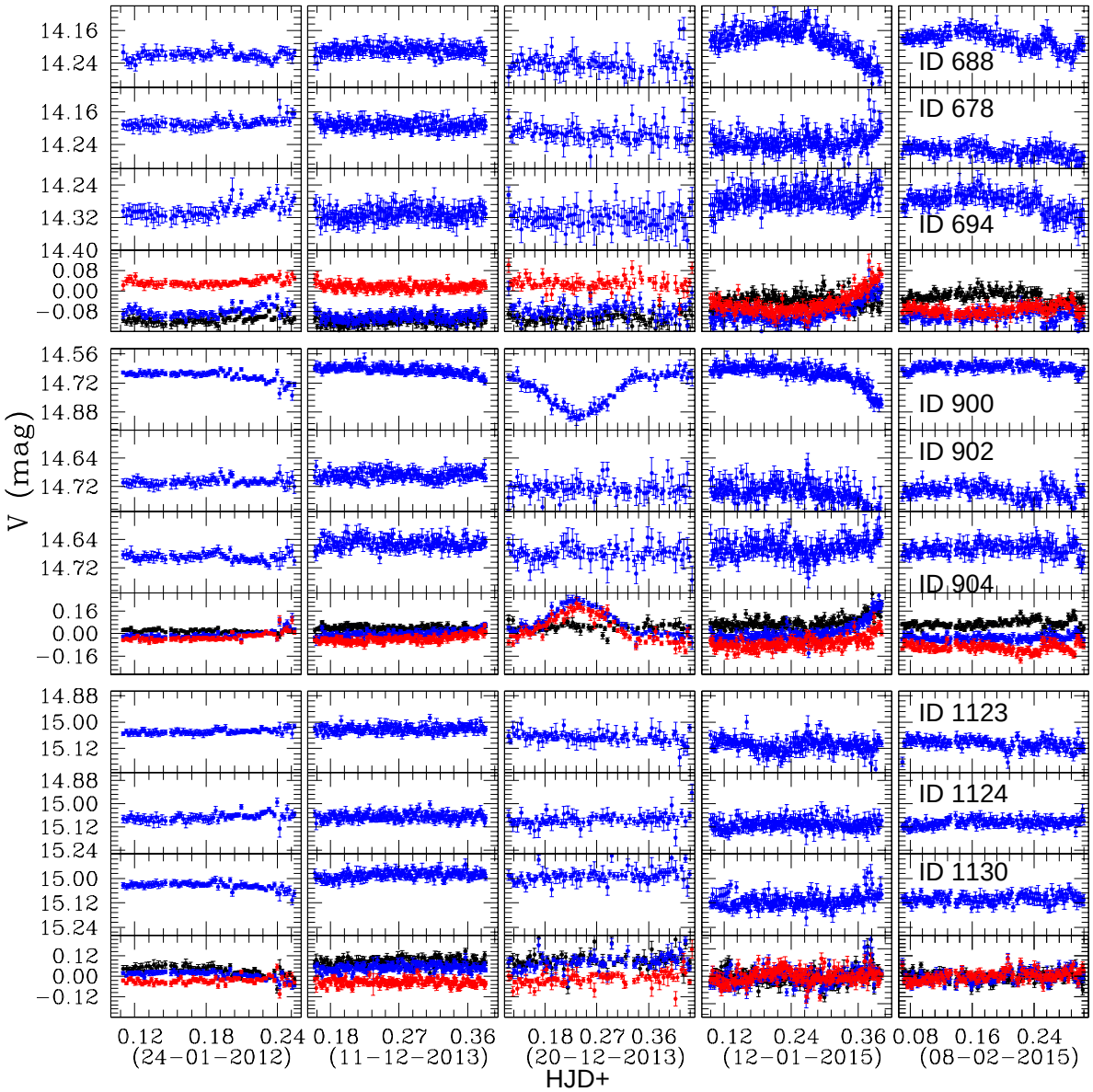

Fig. 5 The panels represent the stellar light curves for star IDs 678, 688, 694, 900, 902, 904, 1123, 1124 and 1130 of cluster NGC 1960. The star IDs 678 and 694 are selected comparison stars for Potential variable (V_4, Star ID 688). The star IDs 902 and 904 are selected comparison stars for Potential variable (V_5, Star ID 900). The star IDs 1124 and 1130 are selected comparison stars for Potential variable (V_6, Star ID 1123).

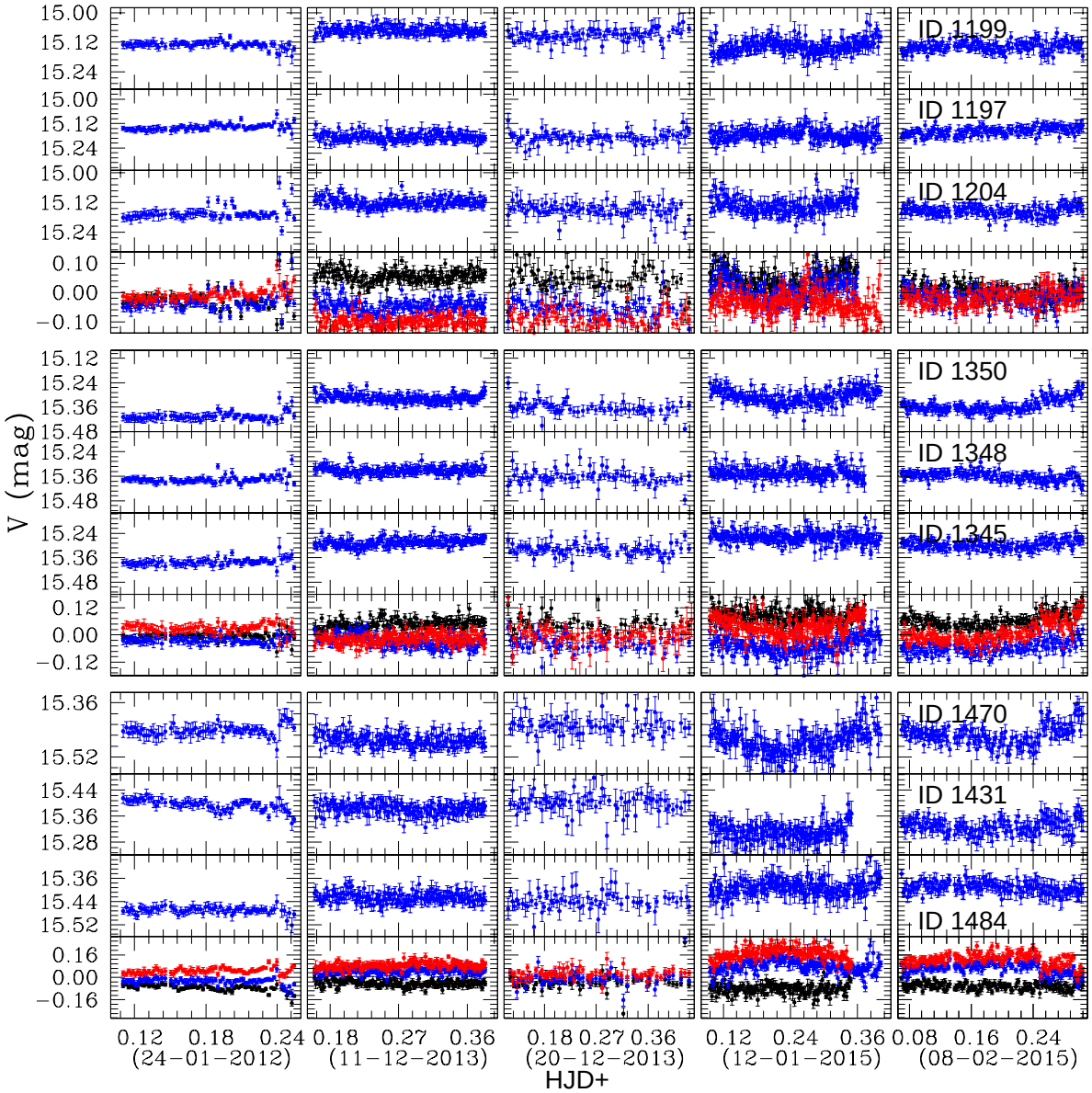

Fig. 6 The panels represent the stellar light curves for star IDs 1197, 1199, 1204, 1345, 1348, 1350, 1431, 1470 and 1484 of cluster NGC 1960. The star IDs 1197 and 1204 are selected comparison stars for Potential variable (V_7, Star ID 1199). The star IDs 1345 and 1348 are selected comparison stars for Potential variable (V_8, Star ID 1350). The star IDs 1431 and 1484 are selected comparison stars for Potential variable (V_9, Star ID 1470).

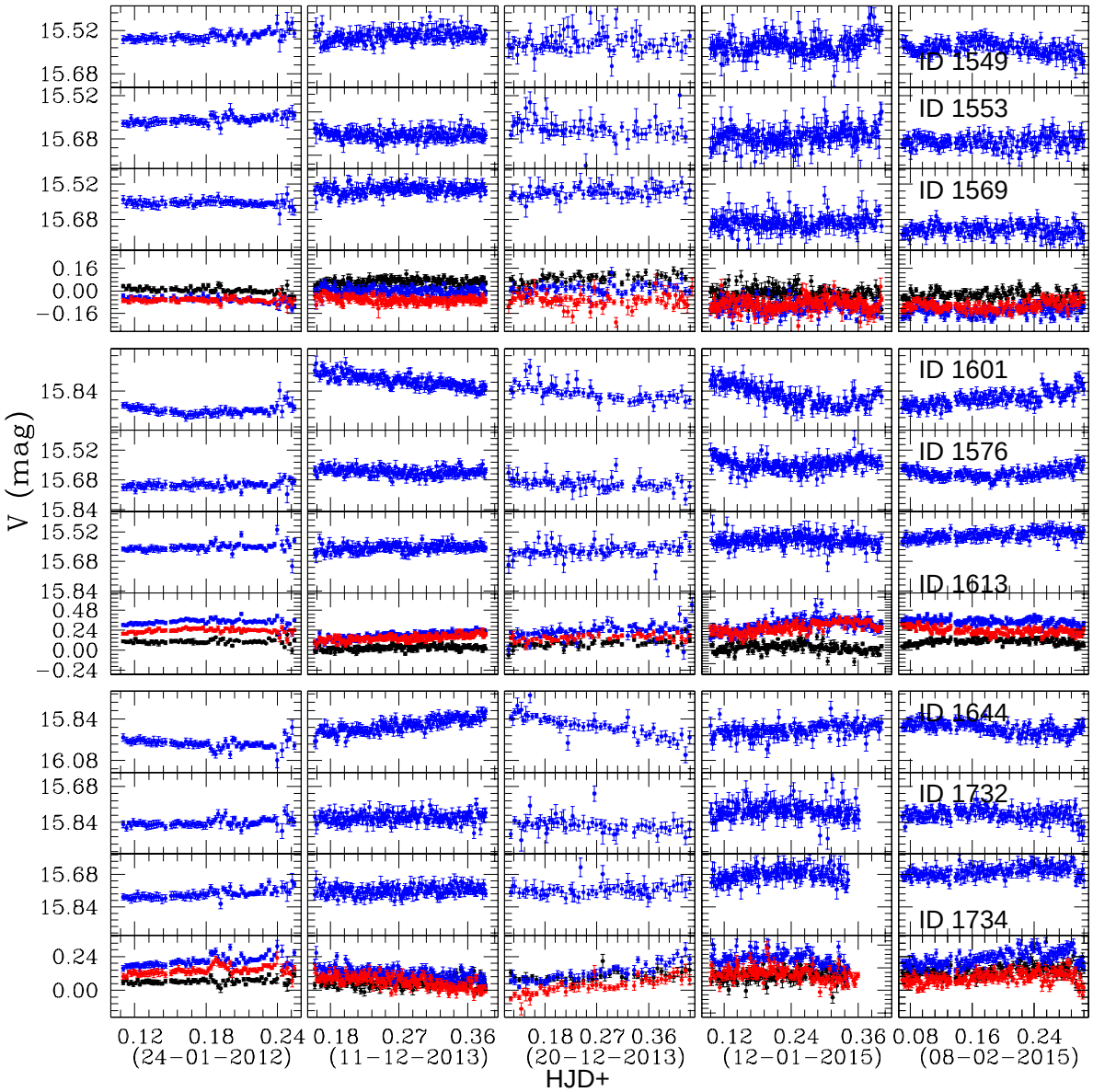

Fig. 7 The panels represent the stellar light curves for star IDs 1549, 1553, 1569, 1576, 1601, 1613, 1644, 1732 and 1734 of cluster NGC 1960. The star IDs 1553 and 1569 are selected comparison stars for Potential variable (V_{10}, Star ID 1549). The star IDs 1576 and 1613 are selected comparison stars for Potential variable (V_{11}, Star ID 1601). The star IDs 1732 and 1734 are selected comparison stars for Potential variable (V_{12}, Star ID 1644).

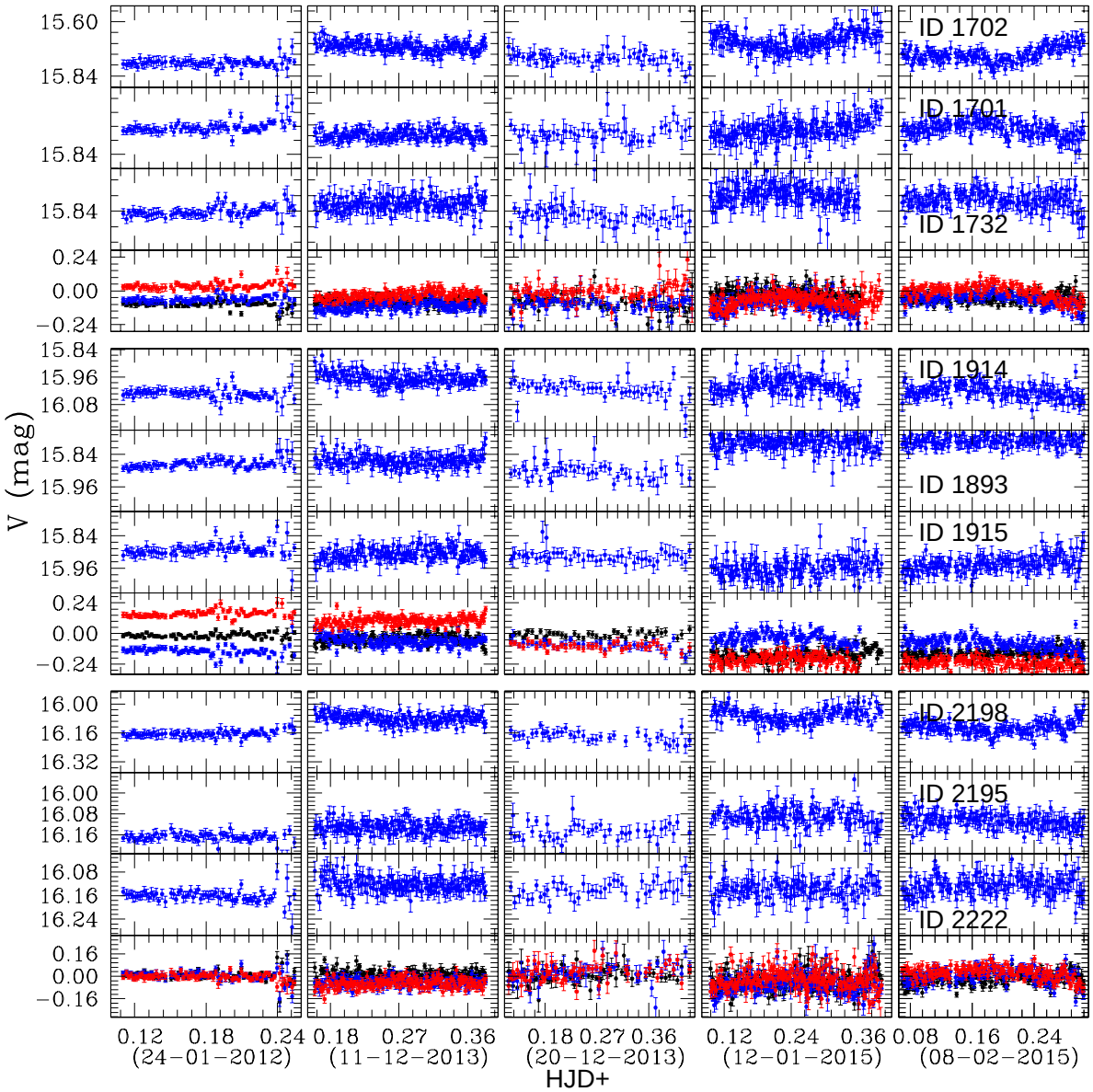

Fig. 8 The panels represent the stellar light curves for star IDs 1701, 1702, 1732, 1893, 1914, 1915, 2195, 2198 and 2222 of cluster NGC 1960. The star IDs 1701 and 1732 are selected comparison stars for Potential variable (V_{13}, Star ID 1702). The star IDs 1893 and 1915 are selected comparison stars for Potential variable (V_{14}, Star ID 1914). The star IDs 2195 and 2222 are selected comparison stars for Potential variable (V_{15}, Star ID 2198).

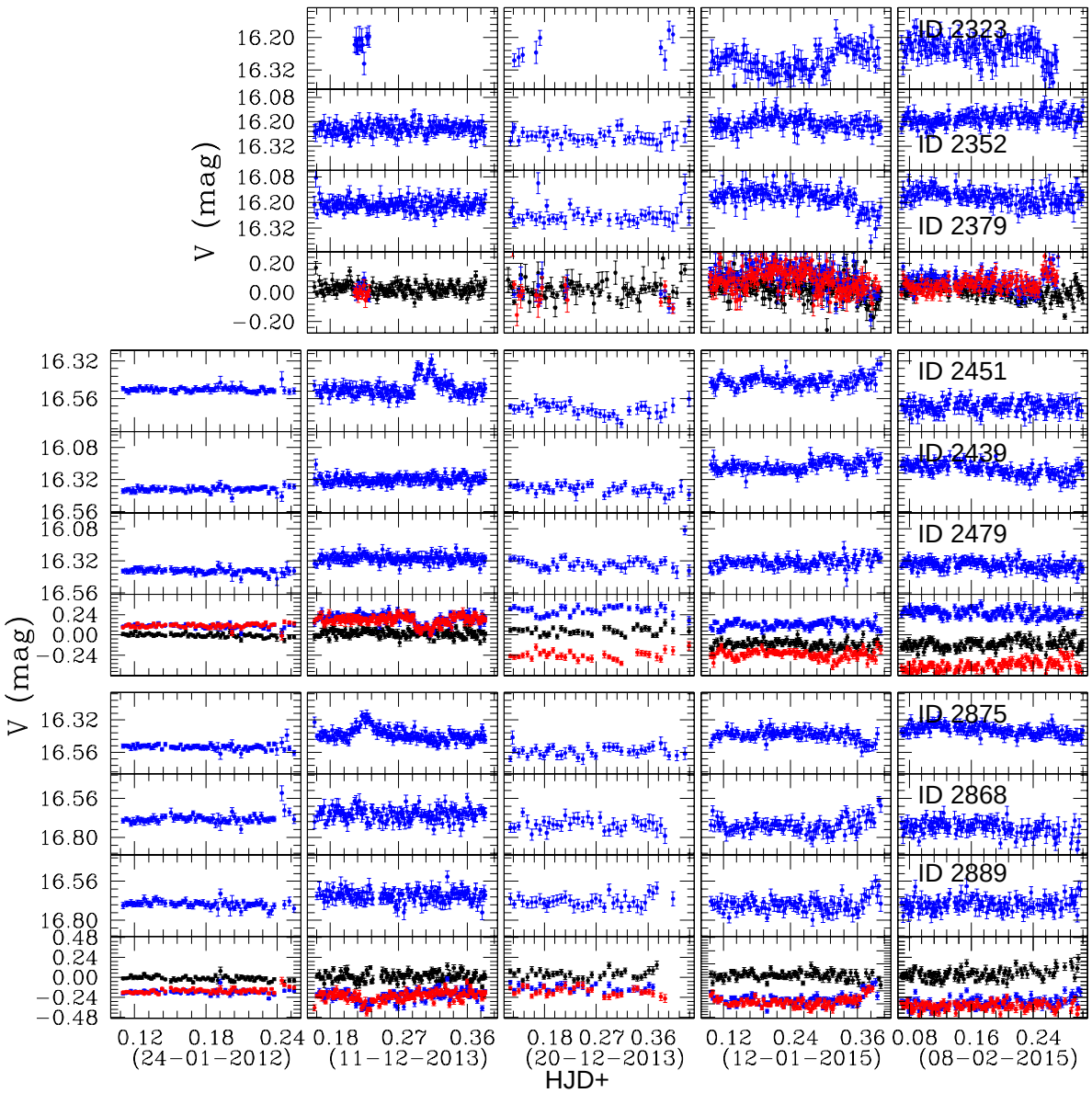

Fig. 9 The panels represent the stellar light curves for star IDs 2323, 2352, 2379, 2439, 2451, 2479, 2868, 2875 and 2889 of cluster NGC 1960. The star IDs 2352 and 2379 are selected comparison stars for Potential variable (V_{16}, Star ID 2323). The star IDs 2439 and 2479 are selected comparison stars for Potential variable (V_{17}, Star ID 2451). The star IDs 2868 and 2889 are selected comparison stars for Potential variable (V_{18}, Star ID 2875).

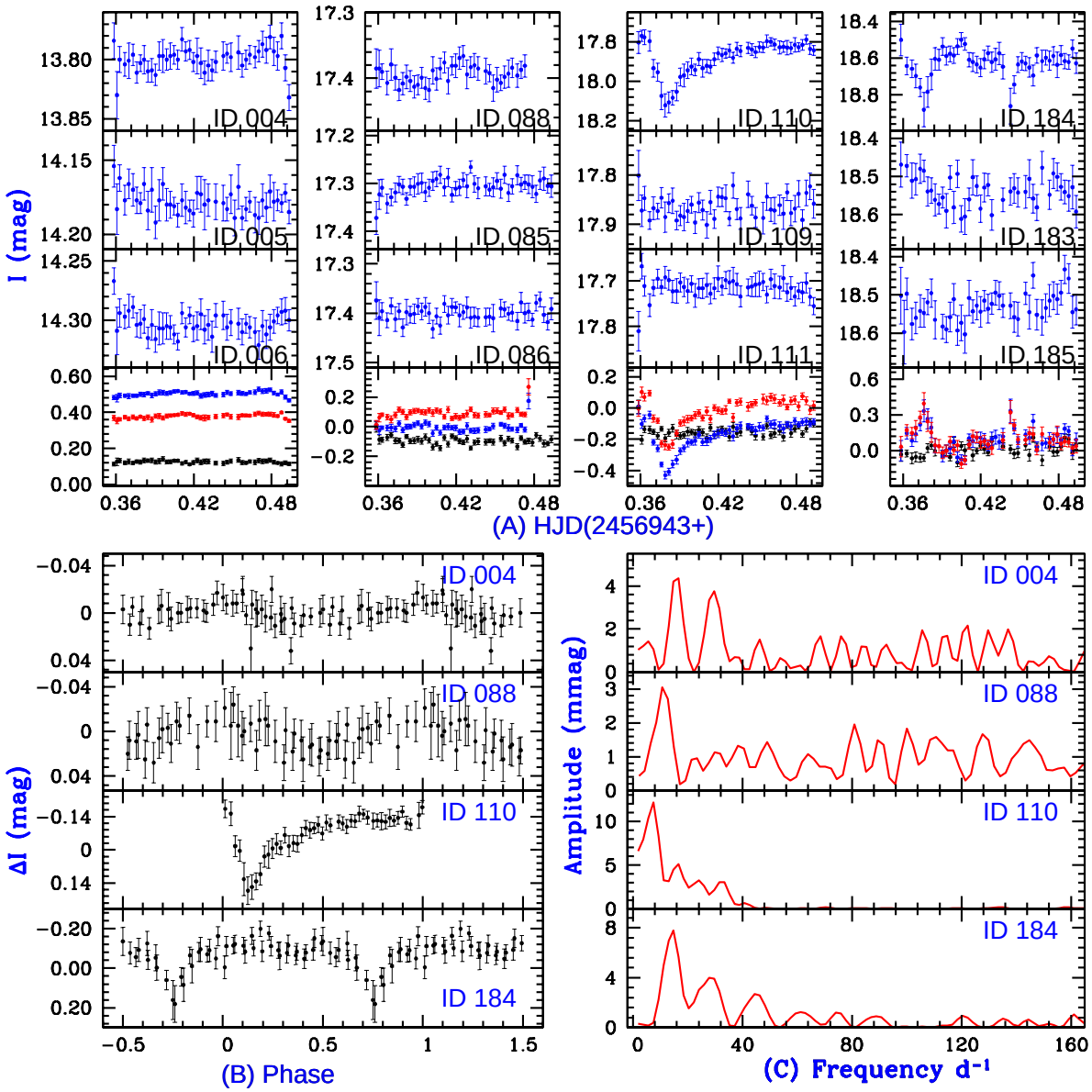

Fig. 10 **(A):-** We represent the light curves of identified varibles (ID 004, ID 088, ID 110, ID 184) and their correspanding comparision stars in the field-view of DOLIDZE 14. The HJD time of observations are shown in x-axis whereas y-axis is shown apparent magnitudes of stars in I-filter. **(B):-** The panels show light-pholded-curves or phase diagrams of identified variables. The value of phase and amplitude ($mmag$) of stellar variability are shown in the x-axis and y-axis respectively. **(C):-** The frequency spectrum of identifed varaibles of DOLIDZE 14 are depicted here. The frequency (d^{-1}) and amplitude ($mmag$) of variables are represented in x-axis and y-axis respectively.

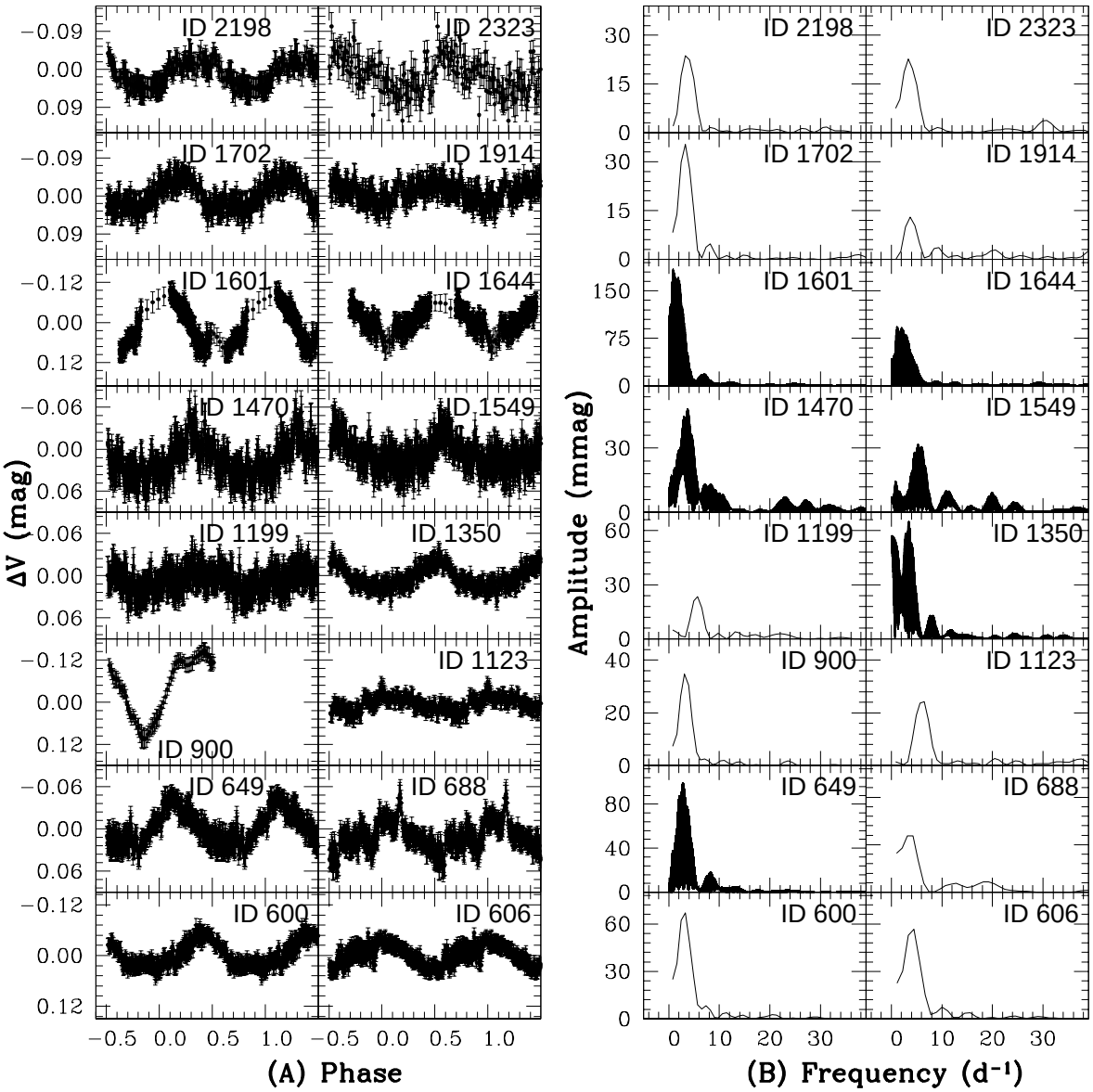

Fig. 11 The left panels represent the phase-folded-diagrams of identified variable stars within the cluster NGC 1960, whereas their corresponding DFT represent in the right panels.

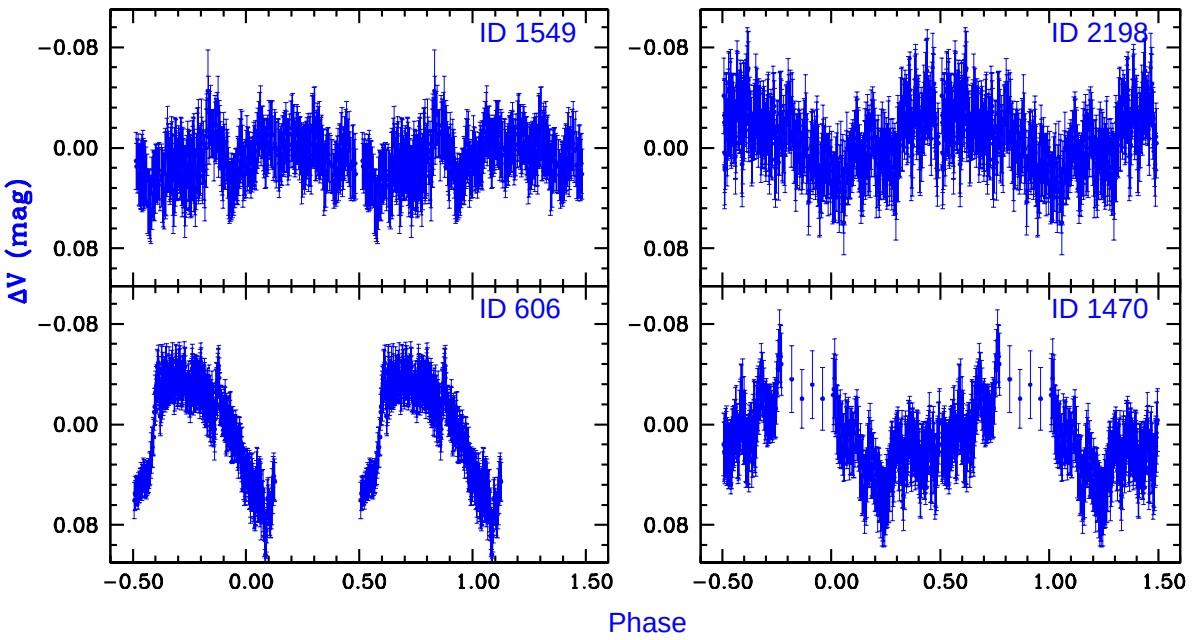

Fig. 12 The panels represent the phase-folded-diagrams of variable stars of cluster NGC 1960 as per period via ANOVA.

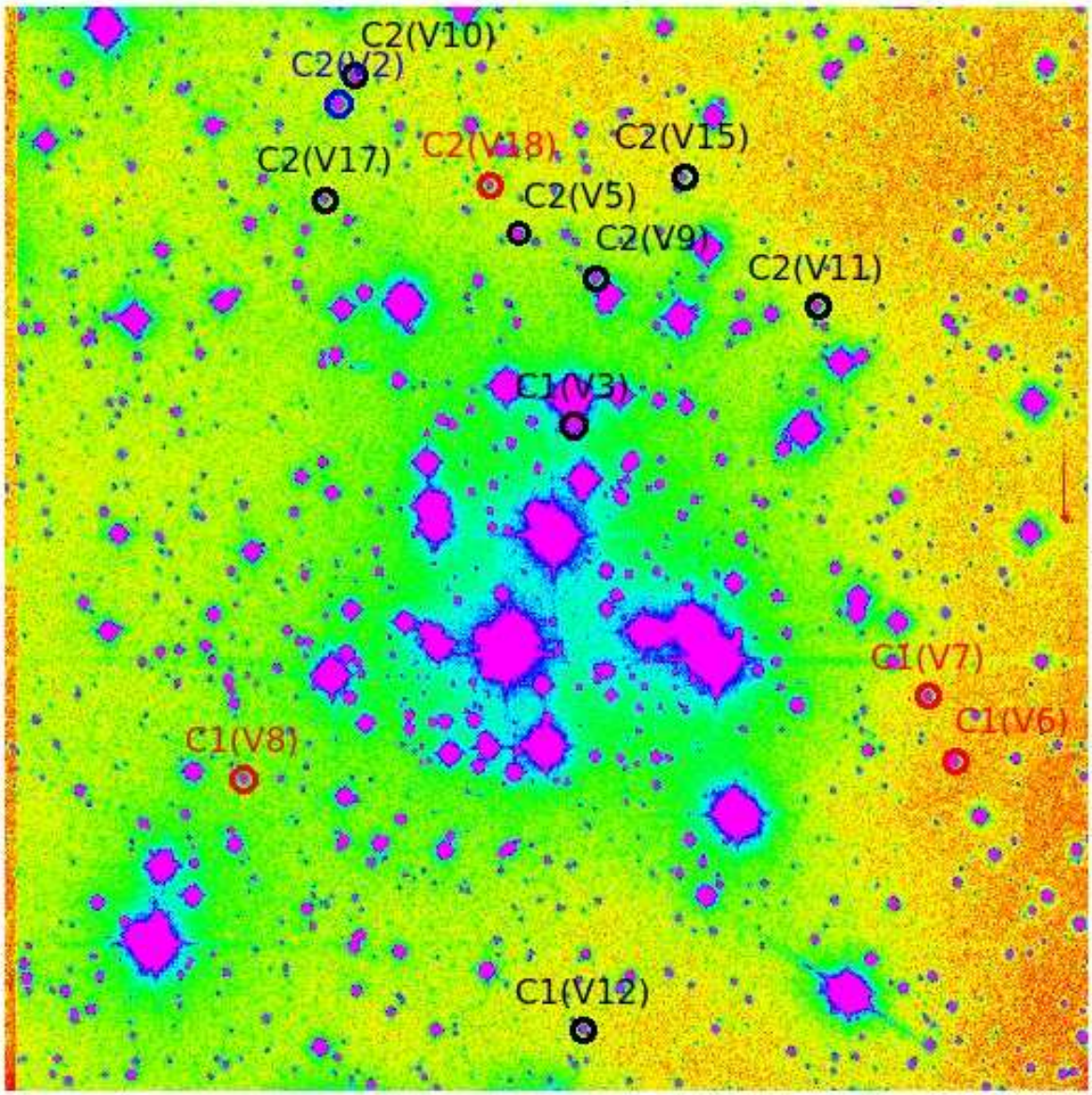

Fig. 13 The finding chart for selected comparison stars within cluster NGC 1960. Identified standard stars are marked by red open circles and they have almost constant brightness/flux during observations. Black open circles represent those long periodic variable stars, for which approximate flux is found for a particular night of observation. However, the value of magnitude is varying nigh to night.

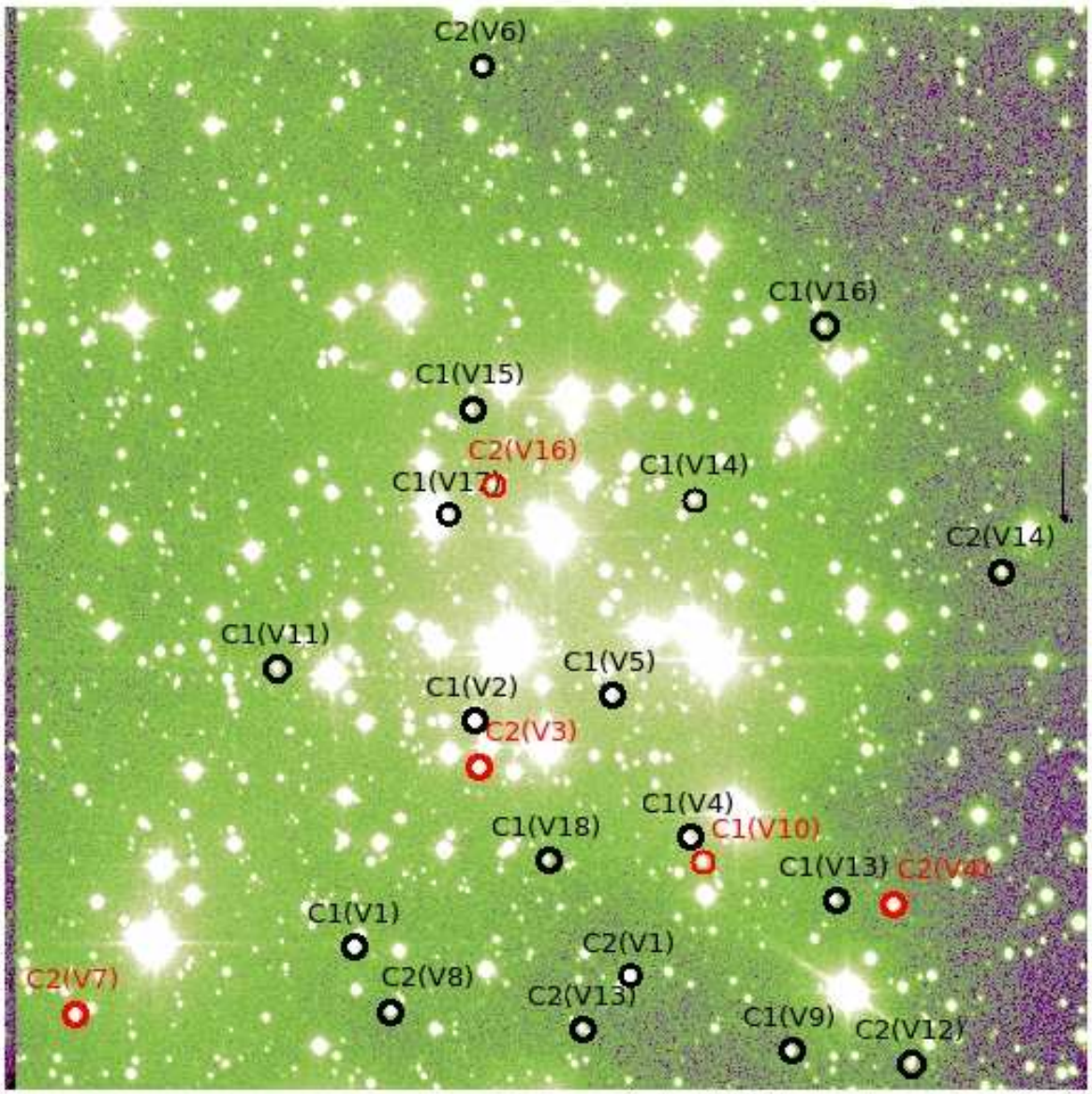

Fig. 14 The finding chart for selected comparison stars within cluster NGC 1960. Red open circles represent those Long term variable stars, for which variation in brightness is also found as daily basis. Black open circles are depicted stars that have irregular flux variation in their light curves as extracted through absolute photometry.

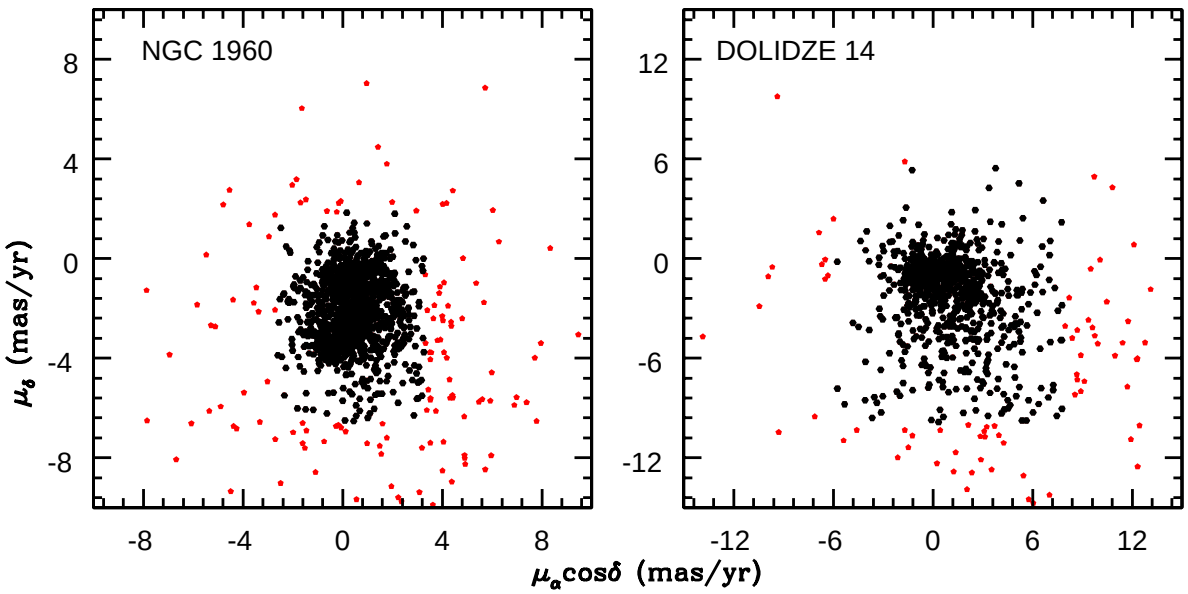

Fig. 15 The distribution of proper motion of stars present in the cluster region. The large points represent those stars which are used to determine the mean proper motion of the cluster.

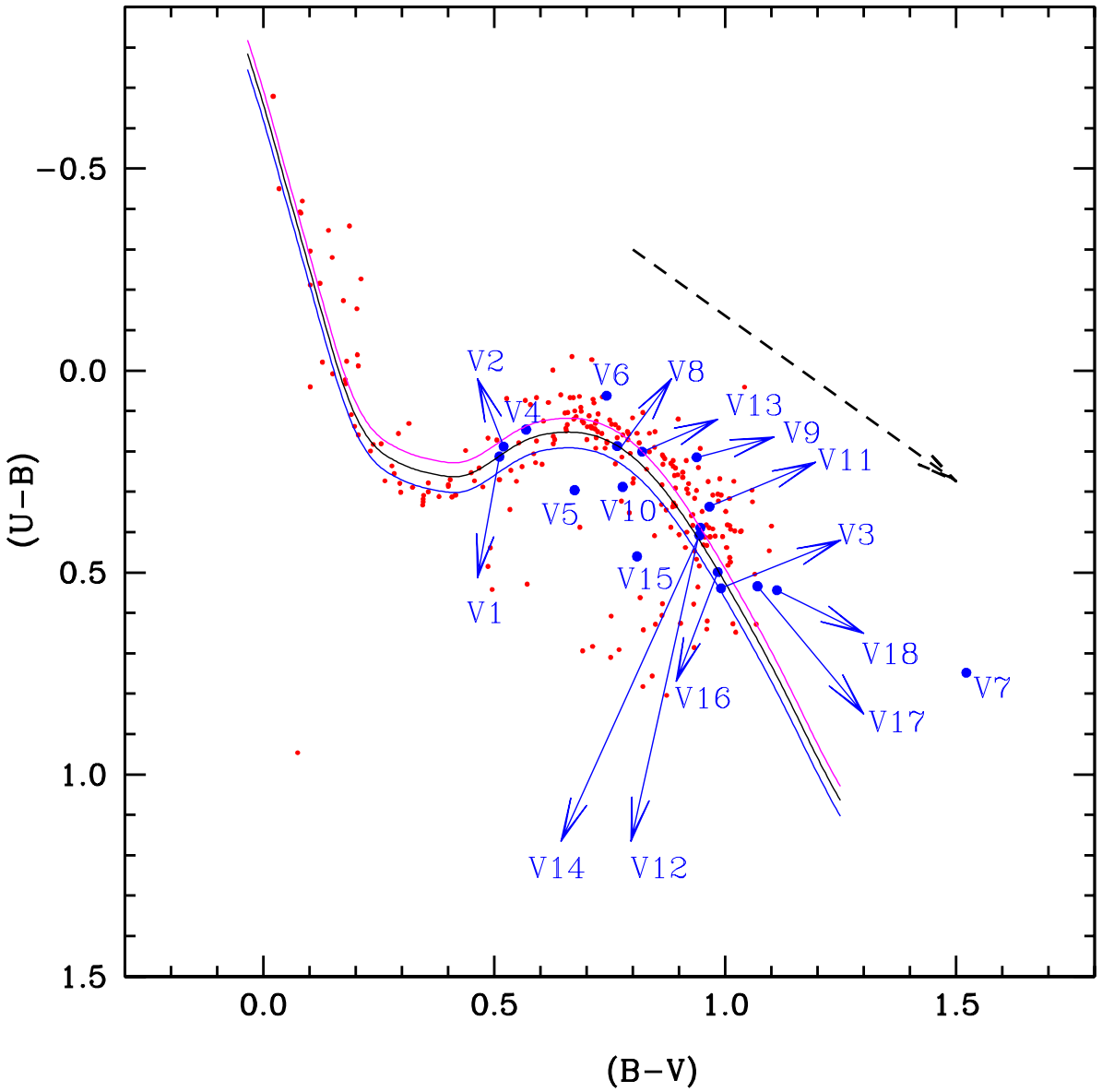

Fig. 16 $(B-V)$ vs $(U-B)$ colour-colour diagram for the MPMs in the field of cluster NGC 1960 as per Joshi & Tyagi (2015). For clarity, variable stars of NGC 1960 are represented by blue dots. The dotted black arrow shows a slope of normal reddening vector $E(U-B)/E(B-V)$=0.72. The solid black line shows the best fit taken in account of 0.23 and 0.17 mag shift in $(B-V)$ and $(U-B)$, respectively while pink and blue lines represent an error of ±0.15 in the reddening vector respectively.

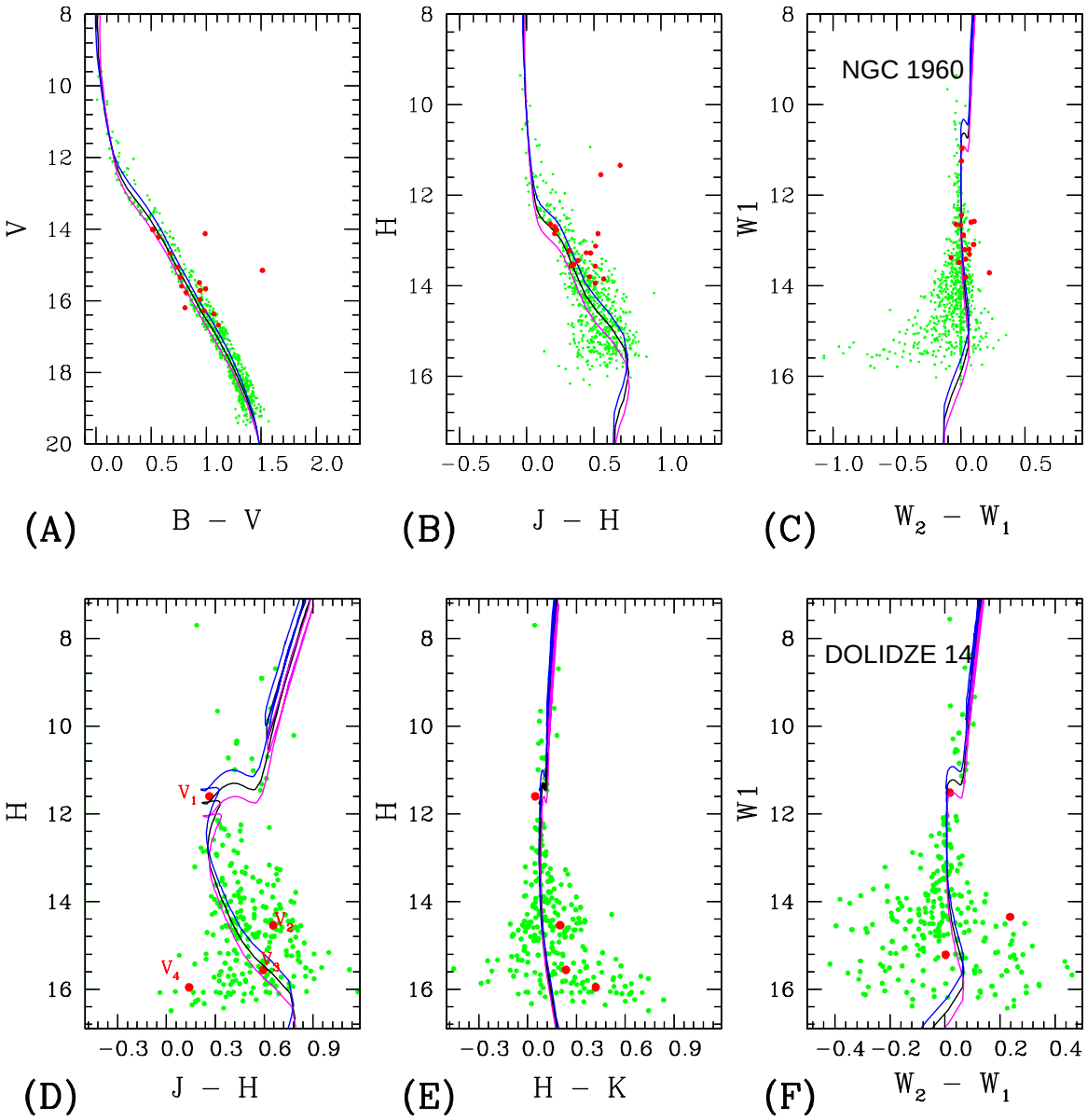

Fig. 17 The upper and bottom panels of this figure represent CMDs for NGC 1960 and DOLIDZE 14, respectively. The red dots on each panel represent the variable stars as identified by us through the time series photometric data while green dots represent the probable members of the studied clusters as extracted from the work of Joshi & Tyagi (2015) and Joshi & Tyagi (2015b). The black solid lines represent the best fitted theoretical isochrones as given in the previous studies. In the panel **16 (A)**, there are no variable stars situated near the turn-off region of NGC 1960 due to selected magnitude range (13.17±0.30 *mag* to 16.61±0.30 *mag*) in V-band. In the case of no prerequisite criteria of magnitude, detected variable stars should be found simultaneously everywhere including (turn-off region) as depicted for DOLIDZE 14 in the panel **16 (D)**.